Ultraviolet Light Surface Treatment as an Environmentally Benign Process for Production, Maintenance and Repair of Military Composite Structures

Project # PP-1182

FINAL TECHNICAL REPORT
February 28, 2002

Professor Lawrence T. Drzal
Department of Chemical and Materials Engineering
Composite Materials and Structures Center
Michigan State University

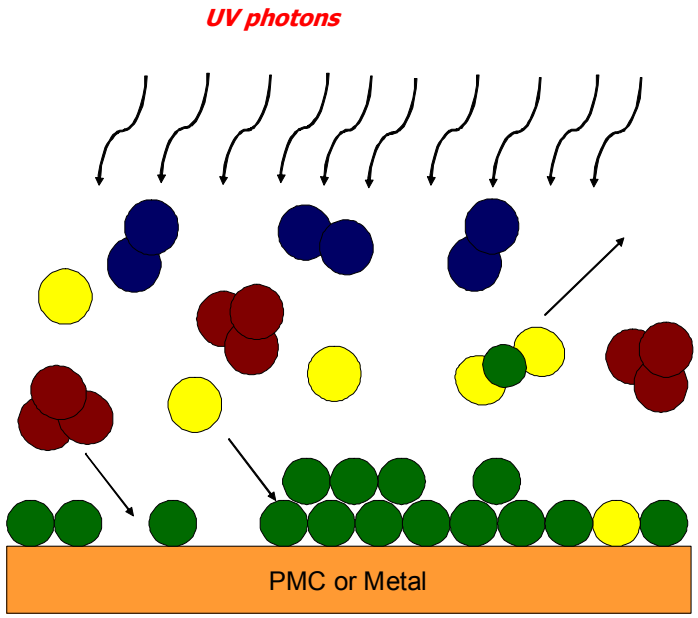

Project Title

ULTRAVIOLET LIGHT SURFACE TREATMENT AS AN ENVIRONMENTALLY BENIGN PROCESS FOR PRODUCTION, MAINTENANCE AND REPAIR OF MILITARY COMPOSITE STRUCTURES

Performing Organization

Professor Lawrence T. Drzal
Department of Chemical and Materials Engineering
Composite Materials and Structures Center
Michigan State University
East Lansing, MI 48824

Project Background

It has been discovered that exposing surfaces of different PMC materials to UV radiation of appropriate wavelengths in air under varying processing conditions has the potential to be a new low-cost, high-speed, environmentally benign, dry surface treatment method for production and repair of military composite structures. It was discovered in the early 1970's that UV light in combination with atmospheric oxygen "cleans" surfaces. This takes place when UV light in the 180-320 nm wavelength region interacts with atmospheric oxygen and creates ozone which decomposes to nascent oxygen and oxidizes surface organic molecules and contaminants to carbon dioxide and water. We have been investigating the use of special UV lamps to treat a variety of thermoset and thermoplastic polymer surfaces. The energy of the UV photons is sufficiently high to break certain surface bonds in the polymers and polymer composites. The nascent oxygen created reacts at the sites of broken bonds to form polar functionality's like hydroxyl, carboxyl, etc. Thus while the substrate surfaces are being cleaned, the chemical characteristics of the treated surfaces are also being changed resulting in a high surface energy. The resultant surface has beneficial chemistry for adhesive bonding or painting purposes. No other solvents, solutions or chemicals are used in this process, the treatment times are on the order of seconds and if done properly, the effect lasts for hours or days. Since this is a surface reaction with ozone created only between the lamp and the PMC surface, very little ozone is generated requiring no special pollution abatement steps. Shielding of UV from workers can be readily accomplished with standard industry methods. Thus UV oxidation and surface treatment has the potential for being a low cost, fast robust method for surface preparation of a wide range of substrates for adhesive bonding or painting purposes. An added benefit is that very large complex and convoluted shapes can be treated in air without the requirement of special chambers or environments or the large capital investment associated with such facilities.

Objective

The principal objective of this work is to develop a low-cost, high-speed, environmentally benign, dry surface treatment method for production, and repair of military composite structures using ultraviolet (UV) light in ambient air. The potential advantage of this method is that it would eliminate volatile organic wastes (VOC's), reduce or eliminate the use of solutions and detergents, and provide a robust surface that would enhance or eliminate the use of solutions and detergents, and provide a robust surface that would enhance the wetting and spreading of paints, coatings and adhesives on polymeric

and inorganic surfaces treated by this method. A manufacturing base for UV production equipment is in place although not for this application.

There is a need for development of an environmentally friendly, cost effective as well as a robust surface treatment method that can clean a surface as well as create a beneficial chemistry for painting and produce optimum adhesive bonding of polymers, polymer composites and metal surfaces. With this in mind, three main technical objectives were sought in this work. The first objective was to determine the usefulness of UV and UV/O_3 to surface treatments to clean and chemically modify the surface of typical PMCs used in DOD systems. The second objective was to determine the effectiveness of this surface preparation for production and/or repair of adhesively bonded, painted and/or coated polymer matrix composite structures. Finally, a determination of the environmental and performance benefits of this method as a new environmentally benign processing method for the production and/or repair of adhesively bonded, painted and/or coated composite structure.

Technical Approach

The technical approach proposed here is based on sound adhesion science principles and reflects the connection between surface preparation with the adhesive joint fabrication and performance whether for new structure or repair. The emphasis will be on adhesively bonded structure, however, the utility and benefits of this method can be extended to adhesion of paints and coatings to PMC surfaces as well.

Structural adhesive bonding of polymer composite parts is an attractive fabrication method. When properly done, adhesive joining creates strong stable joints with superior mechanical and durability characteristics to mechanically fastened structures. There are several models that describe adhesive bonding. The mechanical interlocking model describes the keying or interlocking of the adhesive into cavities and pores of the adherend as a major constituent of the adhesive bond strength. Intrinsically, the effect of surface roughness is significant in determining the adhesive strength. The thermodynamic model is based on the theory that adhesion occurs because of interatomic and intermolecular forces between the adherent and the substrate. London forces, van der Waals forces, and Lewis acid-base interactions are the most common interfacial forces. Another important, but not always necessary, criterion for good adhesion is good solid-liquid contact, or wetting, of the adhesive to the surface. Wetting is typically evaluated by measuring the equilibrium contact angle. When the contact angle is zero, the liquid completely wets the solid and spontaneously spreads over the surface. The chemical bond model describes the interaction between the adhesive and surface as the formation of ionic or covalent bonds between the two materials. Ionic and covalent bonds have bond strengths on the order of 100 to 1000 kJ/mole, much stronger than those observed for the secondary forces described previously.

Preparation of the surface, in addition to choosing the proper adhesive, is an important step in joining two materials. The surface must be cleaned to remove grease, oils, and compounds such as mold release, which can hinder the bonding process. Likewise the surface may need to be chemically modified to remove labile organic compounds and add chemical functional groups to the adherend surface that can interact strongly with the adhesive. Mechanical surface treatments (e.g., abrasion) are currently used as surface preparation techniques but are time consuming, labor intensive, and can damage the polymer adherend surface. Furthermore, organic solvents used for surface preparation also are being eliminated in order to reduce volatile organic compounds (VOC) emissions.

The preferred surface treatment method would both clean a surface as well as create a beneficial chemistry for optimum adhesive bonding of polymer composites. This takes place when ultraviolet (UV) light interacts with the polymer surface. Bond strengths for carbon bound to oxygen, nitrogen, and halogens, as well as alkenes, alkynes, and aromatic systems typically range from 300 to 600 kJ/mole.

Short wavelength photons (λ<365 nm) are of sufficient energy to break many of these bonds. Indeed the interaction of photons with polymers may result in chain scission or crosslinking. Additionally, the thermal energy generated from absorbed infrared radiation or due to the electronic relaxation of a molecule following absorption of a photon can induce melting at the polymer surface.

Surface preparation of the adherend is the keystone upon which the structural adhesive bond is formed. As an example, the nature of the matrix in carbon fiber-reinforced polymeric composites precludes conventional methods of joining, such as riveting and bolting. The preferred method to date is adhesive bonding or adhesive bonding in the presence of a bolt. To achieve maximum bonding a surface pretreatment on the epoxy composite is generally performed. Common composite surface pretreatments include grit blasting, peel ply and chemical etch.

Summary of Project

Task 1: To investigate the use of UV light treatment in air to clean and modify the surface of the typical PMCs used in DOD systems. In the first task we will select up to 2 thermoplastic (e.g., PEEK, PEKK) and 4 thermoset polymer matrix composites (e.g., 3501-6, AFR700, etc.) representative of structural systems in use or planned to be in use in DOD applications in the near future. Pulsed UV treatment will be applied and conditions optimized in order to determine the effectiveness of the UV treatments.

Task 2: To determine the effectiveness of this surface preparation for production and/or repair of adhesively bonded polymer matrix composite structure. The second task will involve fabrication of adhesively bonded joints. PMC surfaces will be prepared with optimized pulsed UV treatments according to the results in Task 1. Two different commercial adhesives, such as Cytec FM-123 and FM-300, and one model epoxy adhesive will be used. Test specimens are expected to include double lap shear (ASTM D5868-95), Mode I fracture toughness (ASTM D5528-94a) and the wedge test (ASTM D3762-98). Fracture surfaces will be preserved and the chemistry will be analyzed with XPS and the fracture surface morphology will be determined using the ESEM.

Task 3: To determine the environmental, cost and performance benefits of this pulsed UV method as a new, environmentally benign processing method for the production and/or repair of adhesively bonded, painted and/or coated composite structure. Once the optimum processing conditions have been determined from the results of Tasks 1 and 2, appropriate analysis procedures will be undertaken for the estimation of the cost of implementing this method for production and repair. Standard chemical engineering process estimation methods will be used.

Project Accomplishments

Introduction

In the application of pulsed UV surface treatment to composite production or composite repair, proper irradiation parameters combined with surface and mechanical property characterization are critical to a fundamental understanding how the pretreatment affects adhesion. The objective of a production action is to fabricate the composite structure with physical and mechanical properties to achieve specified design levels with a high degree of certainty. The objective of a repair action is to restore the physical and mechanical properties of a composite component and allow it to function in its operational environment. In the best case, composite repair would utilize material similar to that of the original structure. The integrity of the adhesive bond is the key factor in attaining the desired performance level in both situations. When considering bonded composite repair, it is important to categorize the severity of damage into three categories: nonstructural, secondary structural, and primary structural repairs.

Nonstructural damage includes gouges, scratches, dents, or other defects that are confined to the surface of the composite laminate. Such damage types can be dealt with by utilizing "cosmetic" repair techniques. Secondary structure can be thought of as those components on which flight dependence is not critical. Strength is not a critical factor with such components. The primary objective for these cases is restoration of stiffness or stability. Precured, cocured, and wet patches, can be used for such repairs. Primary structure is that part of the airframe which is critical for flight. Two types for bonded

primary structural repair; a scarf repair and an external patch repair. Abrading the damage surface and solvent wiping aids in enhancing adhesion and helps ensure some degree of longevity.

The processing requirements of thermoplastic composites pose new challenges to repair technology developments. In addition to the higher temperature requirements, high pressures are also required to melt and consolidate the prepreg. The thermoplastic repair sequence involves fabrication of the composite patch, forming of the patch to the shape of the damaged area, and bonding of the patch to the structure. Surface preparation of the adherend is the foundation upon which the structural adhesive bond is formed. To achieve maximum bonding a surface pretreatment on the epoxy composite is almost always required. Common composite surface pretreatments include grit blasting, peel ply, and chemical etch.

In this work ultraviolet light treatment of both thermoplastic and thermoset materials for the enhancement of adhesion of both composites and damaged composites will be performed. To achieve the necessary scientific understanding, composites will be treated with UV and UV combined with supplemental ozone. The surface chemistry will be examined using contact angle analysis and x-ray photoelectron spectroscopy. The adhesive properties of the UV treated materials will be investigated by mechanical testing. In addition, a model thermoplastic material (polycarbonate) will be extensively tested in an effort to optimize the UV treatment process.

Experimental Methods

Materials. The materials studied consisted of an AS-4/3501-6, $[0, 90]_s$, 6 ply carbon fiber/epoxy composite acquired from Naval Air Warfare Center, Aircraft Division. This is a general purpose structural composite where the 3501-6 epoxy is an amine-cured resin. It will retain a light tack for a minimum of 10 days at room temperature. The panel was intentionally aged for over 2 months before UV treatment. The composite panel was autoclave cured at 240ºF for 1 hour then 350ºF for 2 hours with no bleed. The carbon fiber was a plain weave fabric with an areal weight of 19.3 g/m2, with a typical cured resin content of 37-41%. AS-4 carbon fibers are continuous fiber derived from PAN precursor surface treated to improve handling characteristics and structural properties. IM7/977-2, 4 plies, $[0, 90]_s$ 977-2 carbon fiber/epoxy composite acquired from Wright Patterson Air Force Base, Materials Directorate. IM7 carbon fibers (PAN based Hexcel Corp.) with a fiber diameter of 5 μm. The automotive clearcoat (acrylic melamine formulation) painted on steel and thermoplastic polyolefin panels used in this study were cured at nominal schedules. Commercial aircraft panels of stock aluminum and phosphoric anodized aluminum coated with epoxy were used to investigate the effects of contamination and UV treatments. In addition, a commonly used AS-4 carbon fiber/epoxy (diglycidyl ether of bisphenol–A, DGEBA) composite was investigated. Finally, a model thermoplastic material — GE 8040 polycarbonate— was UV treated and analyzed.

UV Lamp Systems. Three UV lamp systems: RC-500B, RC-740, and an RC-747 from Xenon, Corp. (Woburn, MA) and one Equip 6000 system from Fusion UV Systems, Inc. (Gaithersburg, MD) were used to perform UV treatments. A comparison of the details of each of the systems is shown in Table I. The RC-500B system has a pulse frequency of 120 Hz and a 0.3kW output lamp with a coverage area of approximately 5 square inches. The RC-740 has an output power of 1.5 kW and a factory set pulse frequency of 10 Hz with a pulse width of 200 μs and a lamp area of 9.6 square inches. In contrast to these two fixed-frequency systems, the RC-747 has a variable pulse frequency ranging 3 Hz to 120 Hz with a constant pulse width of 200 μs and a variable lamp irradiation area. (The lamp irradiation area results from the optics of the lamp assembly. In the case of the Xenon systems the lamp reflector is

parabolic resulting in a parallel light rays. In contrast, the Fusion system has an elliptical reflector that results in a focused output.) Each UV system was outfitted with a xenon/quartz light source that produces a broad spectrum of high intensity pulsed light in the wavelength range of 190 nm to 1000nm. The lamp-to-sample distance was 5.08 cm in all cases. In some cases supplemental ozone was supplied to substrate surface during irradiation using medical grade oxygen flowing through an ozone generator.

Table I. UV Lamp System Comparison

	RC-500B	RC-740	RC-747 (120 Hz)	RC-747 (3 Hz)	Fusion Equip 6000
Pulse Frequency (Hz)	**120**	**10**	**120**	**3**	**Continuous**
Power Output (W)	**300**	**1500**	**2000**	**2000**	**6000**
Lamp Irradiation Coverage (in.^{2})	**5**	**9.6**	**36**	**36**	**Variable**

Decontamination Studies of Commercial Aircraft Panels. Hand cream and a light forming (hydrocarbon) oil were used to deliberately contaminate the surfaces of epoxy-coated aluminum, phosphoric anodized aluminum and AS4-carbon fiber/epoxy. The hand cream and forming oil was applied liberally to the surface of each material. Kim-wipes (Kimberly-Clark) were used to vigorously wipe off the excess hand cream or oil. Accumulated radiation times are reported. The specimens were passed underneath the UV light by riding on a conveyor belt moving at a speed that allowed a 30 second treatment of each specimen. The samples were allowed to cool to near room temperature after each pass before measuring the contact angle. After measuring the contact angle, the water droplets were removed by wicking the liquid with a Kim-wipe. The previously exposed samples were then re-exposed to the UV light for an additional amount of time. This process was repeated until the sample contact angles remained constant.

Physicochemical Analysis. X-ray photoelectron spectroscopy (XPS) Measurements: The composition and chemical bonding state of the material surface was investigated using a Perkin-Elmer 5400 x-ray photoelectron spectrometer employing a magnesium K_α source and operated at a power of 300 Watts. In general, sample degradation was found to be negligible. A full set of survey scans at a 45º take off angle (approximately 20 minutes) was taken. Comparison of the relative areas of the C 1s peaks from the scans allowed the relative percentages of carbon bonded to oxygen versus carbon not bonded to oxygen. The analyzer was operated at constant pass energy of 20 eV. Line shape analysis was performed on each peak, and atomic percentages were calculated from the peak areas using standard atomic sensitivity factors. All peaks were fitted using a fwhm of 160 eV. The depth of sampling was not determined, but is expected to be approximately 6 nm or less.

Contact Angle Measurements and Surface Energy Calculations: Deionized water contact angles were statically measured using a Rame Hart goniometer Model 100-00-115. An average contact angle was calculated from 10 measurements. Surface energies were evaluated using the surface-tensio-component theory. According to this approach, the surface energy of a solid, γ^s, combines the Liftshitz/van der Waals component, γ^{LW}, the Lewis-acid component, γ^+, and the Lewis-base component, γ^-

$$\gamma_s = \gamma_s^{LW} + (\gamma_s^+\gamma_s^-)^{1/2}$$

For a drop of a liquid at equilibrium with a solid surface, the liquid-solid contact angle (θ) is given by,

$$\gamma_L (1+ \cos\theta) = 2[\gamma_s^{LW}\gamma_l^{LW})^{1/2} + (\gamma_s^+\gamma_l^-)^{1/2} + (\gamma_s^-\gamma_l^+)^{1/2}]$$

where γ_l is the surface tension of the liquid and subscripts s and l, correspond to solid and liquid, respectively. Hence, by measuring contact angles for three, or more, well-characterized (in terms of γ_l^{LW}, γ_l^+, and γ_l^-) liquids three equations with three unknowns are generated. In this work water, glycerol, ethylene glycol, formamide, and diiodomethane were employed as probe liquids.

In addition to the acid-base characteristics of the surface, the thermodynamic work of adhesion, W_A, required to separate a unit area of a solid and a liquid phase forming an interface across which secondary forces are acting may be related to the surface and interfacial free energies by the Dupre equation. The reversible work of adhesion, W_A, in an inert medium may be expressed by:

W_A = (Sum of the surface free energies of the solid and liquid phases – the interfacial free energy)

$$W_A = \gamma_s + \gamma_{lv} - \gamma_{sl}$$

where s, l, and v correspond to the solid, liquid, and vapor, respectively. Note that the value of surface free energy appropriate to the Dupre equation is γ_s, rather than γ_{sv}. The surface free energy may be generally expressed by two terms, namely a dispersion and polar component, such that

$$\gamma_s = \gamma_s^D + \gamma_s^P$$

Where γ_s^D is the dispersion force component and γ_s^P is the polar force component. The proposed relation for interactions involving polar and dispersions forces appears to be a reliable prediction of the interaction energies at the interface. This can be written as

$$\gamma_{ab} = \gamma_a + \gamma_b - 2(\gamma_a^D\gamma_b^D)^{1/2} - 2(\gamma_a^P\gamma_b^P)^{1/2} .$$

Wetting can be quantitatively defined by reference to a liquid drop resting on a solid surface. The tensions at the three-phase contact point are indicated such that lv is the liquid/vapor point, sl is the solid/liquid point and sv is the solid/vapor point. The Young equation, relating these tensions to the equilibrium contact angle, θ, may be written as

$$\gamma_{sv} = \gamma_{sl} + \gamma_{lv} \cos\theta$$

Therefore the work of adhesion can be written as

$$W_A = 2(\gamma_a^D\gamma_s^D)^{1/2} + 2(\gamma_a^P\gamma_s^P)^{1/2}$$

Where the subscripts a and s now represent the adhesive and substrate.

The term γ_{sv} represents the surface free energy of the solid substrate resulting from adsorption of vapor from the liquid and may be considerably lower in value than the surface free energy of the solid in vacuum, γ_s.

Essentially, researchers have accepted the fact that interfacial interactions between polar (Keesom) forces may possibly be predicted from a geometric mean relation, but consider that such interfacial interactions are usually negligible. However, some argue that the polar forces are not always negligible and are reasonably well predicted by the geometric mean relation. Further, the contribution for the acid-base interactions was not always consistent. Thus, choosing between the polar force approach and the acid-base approach is currently difficult. The formation of acid-base interactions between the adhesive and substrate may represent a major type of intrinsic adhesion force that operates across the interface. This classification includes hydrogen bonds that are considered to be a subset of acid-base interactions. The acid may be an electron acceptor, in the Lewis sense, or a proton acceptor, in the Bronsted sense. The base may be an electron donor, in the Lewis sense, or a proton acceptor, in base compatibility: (1) electron acceptors (proton donors, i.e., acids), (2) electron donors (or proton acceptors, i.e., bases), and both electron acceptors (or proton donors) and electron donors (or proton acceptors). For instance, polycarbonate belongs to the second classification and acts as an electron donor.

Debond Strength. The adhesive strength of the treated specimens were tested by two methods. First a single lap shear test measured on specimens (4”x1/2” with an overlap area of 0.375 in.^{2}) using a United Testing Systems load frame operated at a constant crosshead speed of 0.1 in./min. As-received, UV and UV/O_3 treated samples, along with specimens prepared from panels with simulated damage made by abrading with 320 grit sand paper were prepared. Secondly, tensile butt tests were performed using a PATTI (pneumatically activated tensile testing instrument). Five tests were preformed for each treatment condition. In both cases, the adhesive used was a toughened epoxy (Arladite 2015, Ciba) allowed tso cure at room temperature for 24 hours.

*Fractography. F*racture surfaces of failed laminates, both single lap shear and PATTI tests, were examined uncoated using an ElectroScan 2020 environmental scanning electron microscope (ESEM) operating with an accelerating voltage of 20 kV and a water vapor pressure between 2 and 3 Torr.

Results

AS-4/3501-6 Carbon Fiber/Epoxy Composite- Contact Angles

Figure 1 shows the behavior of the water contact angle as a function of treatment time for an AS-

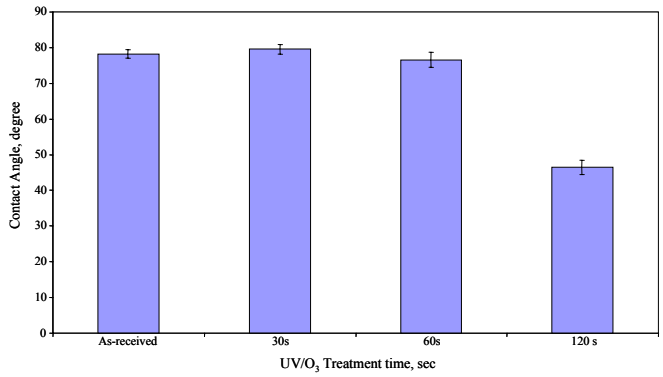

Figure 1: Contact angles as a function of treatment time for the AS-4/3501-6 carbon fiber/epoxy composite UV/O_3 treated using the RC-747 system.

4/3501-6 carbon fiber/epoxy composite that is treated with UV/O_3 using the RC-747 system. The contact angle remains relatively constant for a treatment time of up to 1 minute, but decreases to a value of 45º after treating for 2 minutes. The decrease in contact angle suggests that the epoxy is becoming more hydrophilic as a result of the UV treatment.

Surface Chemistry. XPS analysis of the AS4/3501 control surface, and the UV and UV/O_3 treated surfaces provides a quantitative probe of the functional groups. As Figure 2 shows, the C1s peaks of the AS-4/3501 carbon fiber composite revealed the presence of several functional groups. The C1s peak of the as-received PC is deconvoluted into 4 Gaussian peaks. UV irradiation does not increase

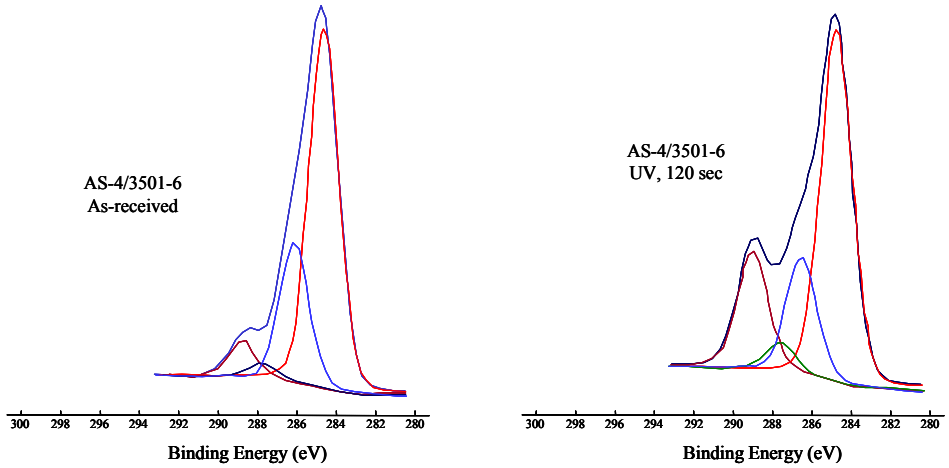

Figure 2: Typical least-squares curve fitting analysis: the C1s spectrum for as-received and UV treated AS-4/3501 carbon fiber composite. (RC-747 system)

the number of deconvolution peaks; however, the intensity of the highest binding energy peak increases significantly.

Details of how the surface treatment affects the surface chemistry are further illustrated by the data presented in Table II. The data indicates that the UV and UV/O3 treatments primarily effect the carbon and oxygen surface concentrations. Other elements, such as nitrogen, silicon, fluorine, and sulfur seem to resist the surface treatments. The amount of carbon decreases approximately 15% after a 5 minute UV treatment and approximately 20% after a 5 minute UV/O_3 treatment. In conjunction with the decrease in carbon, the oxygen concentration increases approximately 45% for a 5 minute UV treatment and approximately 62% for a 5 minute UV/O_3 treatment. In addition to surface treatments performed with the UV lamp on for 30 seconds and then off for 30 seconds, treatments were performed in a continuous manner. These results are listed as 3-minute continuous UV and UV/O_3 treatments. The results for the continuous treatments are comparable to the intermittent treated samples. This indicates that the faster continuous method can be used to treat the composite materials.

Plotting the oxygen-to-carbon atomic ratios allow the identification of trends. The oxygen-to-carbon atomic ratios for both UV and UV/O_3 treated specimens as a function of treatment time are shown in Figure 3. Treating the polycarbonate only with UV causes small gradual increases in the O:C ratio. In contrast, treating with UV/O_3 causes an initial dramatic increase in the O:C ratio after a 1 minute treatment, that seems to plateau at treatment times of 3 and 5 minutes. The atomic ratio data can be further illustrated by plotting the carbon-to-oxygen percent increase as a function of treatment time for UV and UV/O_3 treatments. This data is shown by the plot in Figure 4. The O/C ratio for the UV treated system shows an initial 40% increase after a 1-minute treatment. Increases beyond this treatment time show a linear trend. The percentage increase for the UV/O_3 treated specimens are more dramatic compared to the UV treated specimens. Again, a plateau is observed for treatment times beyond 1 minute.

Table II. XPS data of UV and UV/O_3 treated AS4/3501 carbon fiber/epoxy composite

Sample Treatment	Treatment Time-min.	Carbon	Oxygen	Nitrogen	Silicon	Fluorine	Sulfur	O/C
Control	0	71	21.8	4	0.3	1.9	1	0.307
UV	1	64.7	28.1	4	0.4	1.9	1	0.434
	2	63.5	29.4	4.1	0.5	1.7	0.8	0.463
	3	62.5	30.4	3.1	0.5	2.4	1	0.486
	5	60.7	32	4.4	0.3	1.4	1.1	0.527
UV/O_3	1	60.3	32.6	3.7	0.30	1.9	0.9	0.541
	3	56.8	36.5	3.2	0.5	2.3	0.8	0.643
	5	56.1	35.6	4.8	0.3	1.8	1.5	0.635
Continuous	3 (UV)	62.8	30.8	3.4	0.4	1.8	0.8	0.490
	3 (UV/O3)	57.1	34.9	4.6	0.2	1.8	1.3	0.611

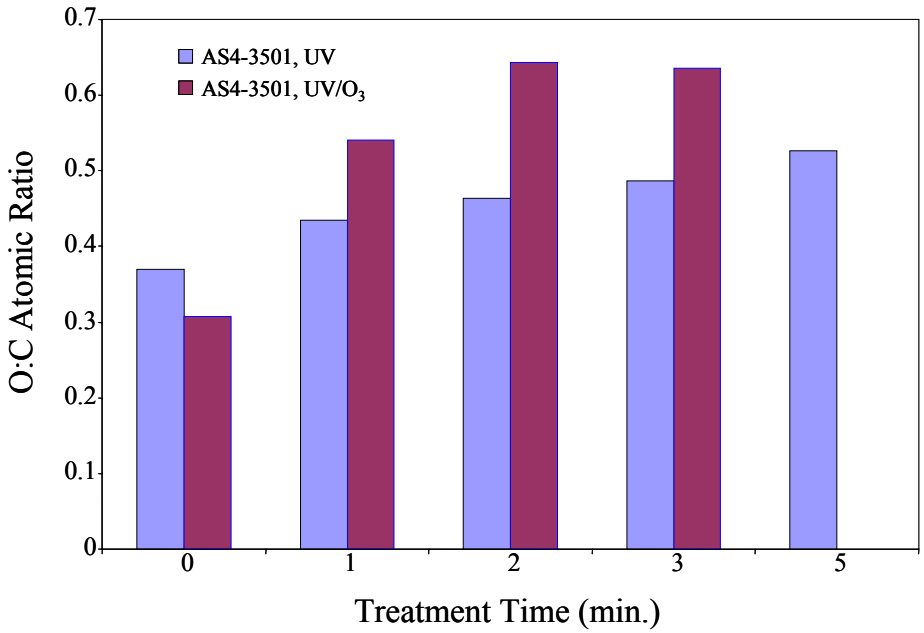

Figure 3: O:C ratios of UV and UV/O_3 treated (RC-747 system) AS-4/3501 carbon fiber composite.

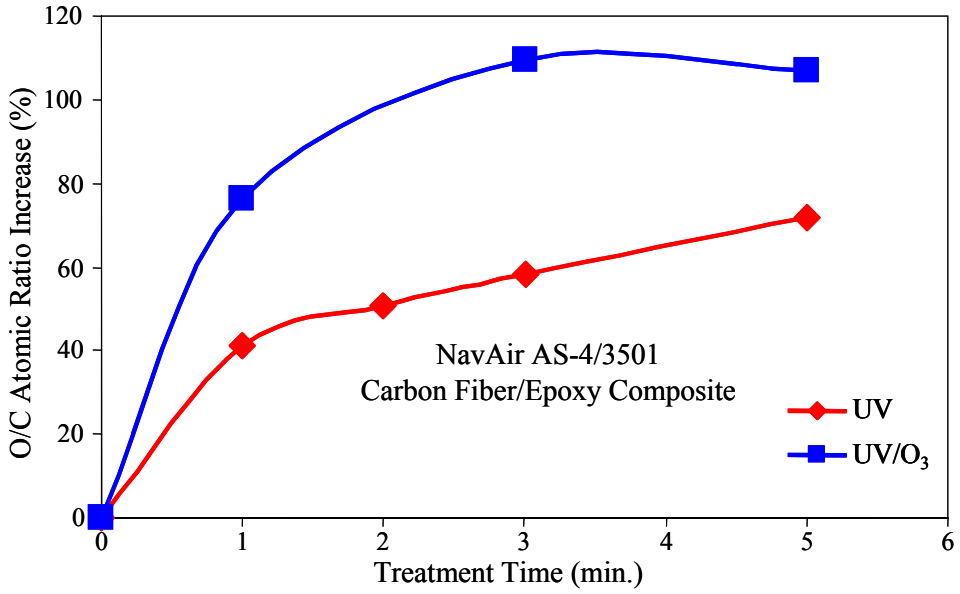

Figure 4: The percentage increase in the O/C atomic ratios for UV and UV/O_3 treated AS4/3501 carbon fiber/epoxy composite.

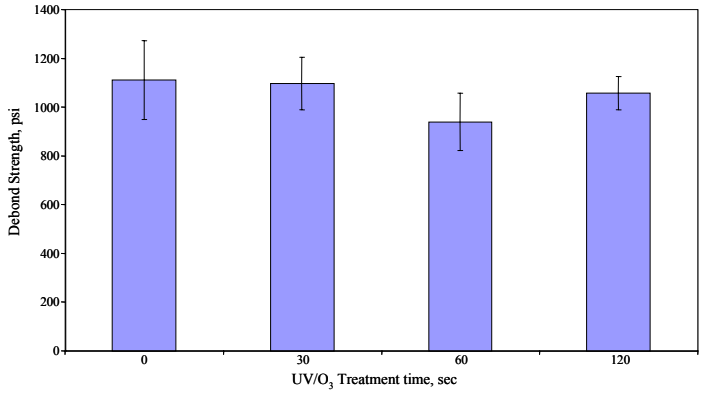

Figure 5: Debond strength of UV/O_3 treated (RC-747) AS-4/3501 carbon fiber composite as measured using a butt tensile test.

The effect of the UV/O_3 surface treatment on the debond strength of is shown by the data in Figure 5. The data indicates that the surface treatment has little, if any, affect on the debond strength of the composite. This null result is interesting since the increased functional group density, combined with increased wettability should provided a good foundation for improved adhesion. One reason for the lack of apparent improvement could be the presence of a large amount of low molecular weight contamination that oxidized, but did not volatized during the UV/O_3 treatment. The low molecular weight material on the surface would act as a mechanically weak interface.

In addition to the tensile butt specimens, single lap shear test coupons were fabricated and tested. The results of these tests are shown in Figure 6. The data indicates slight increases in lap shear adhesion for both untreated and abraded and UV/O_3 treated specimens. A direct comparison between the tensile butt test and the shear lap test is not possible since the applied stresses are different.

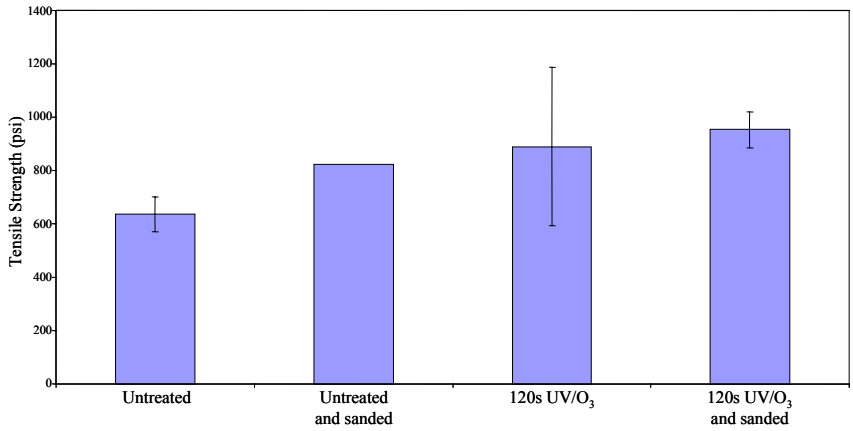

Figure 6: Single lap shear tests for UV/O_3 (RC-747) treated AS-4/3501 carbon fiber composites.

IM7/977-2 Carbon Fiber/Epoxy Composite

The changes in the C1s surface chemistry of untreated and UV treated IM7/977-2 carbon fiber/epoxy composite is illustrated by the data in Figure 7. Reminiscent of the changes created by UV treating the AS4/3501 carbon fiber/epoxy, the majority of the changes taking place after UV treatment

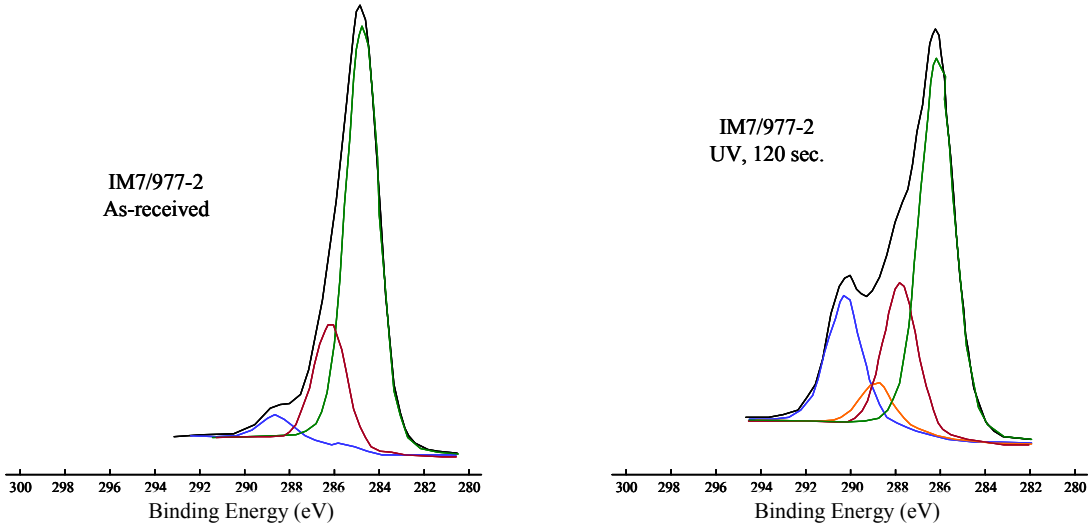

Figure 7: XPS plots of untreated and 120 second UV-treated IM7/977-2 carbon fiber composite specimens using the RC-740 system.

are the increase in the intensity of the high binding energy peak. In addition, to this increase, a new peak appears at a binding energy of 289 eV. The results of the XPS surface chemistry investigation are shown by the data in Table III. Similar to the results for the AS-4/3501 carbon fiber/epoxy composite, the UV treated decreases the carbon concentration and increases the oxygen concentration. The concentration for the nitrogen, silicon, fluorine, and sulfur shows only minor changes. The use of

Table III. XPS data of UV and UV/O_3 treated IM7/977-2 carbon fiber/epoxy composite

Sample Treatment	Treatment Time-min	Carbon	Oxygen	Nitrogen	Silicon	Fluorine	Sulfur	O/C
Control	0	60.4	27.2	2.3	7.6	1.6	0.9	0.450
UV	1	57.8	28.6	1.3	10.2	1.6	0.6	0.495
	2	55.1	31.5	2.3	8.1	1.9	1	0.572
	3	52.5	32.4	1.7	10.8	1.8	0.9	0.617
	5	51.7	34.6	2.9	7.4	1.9	1.4	0.669
UV/O_3	1	53	33.7	2.6	7.9	1.8	0.9	0.636
	2	50.8	37.1	3.3	5.3	2.2	1.2	0.730
	3	47.6	38.2	3	8.1	1.9	1.2	0.803
	5	44.1	41.1	4	7.4	1.7	1.7	0.932
Continuous	3 (UV)	54.3	32.3	2.4	7.4	2.6	1	0.595

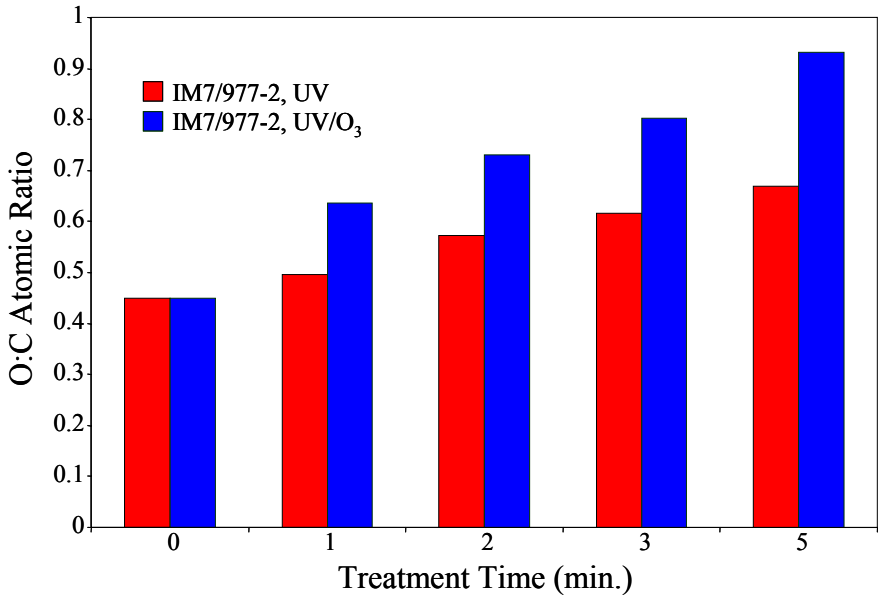

Figure 8: Oxygen-to-carbon atomic ratios as a function of UV and UV/O_3 treatment time for IM7/977-2 carbon fiber composite specimens using the RC-740 system.

supplemental oxygen causes the surface oxygen to increase dramatically compared to the UV treatment. In addition to the expected decrease in carbon, a measurable increase in the nitrogen concentration is observed. As before, the use of a continuous UV treatment has the same effect on the surface chemistry as the intermittent treatment does.

The data in Figure 8 shows how the O/C varies as a function of treatment time. For both

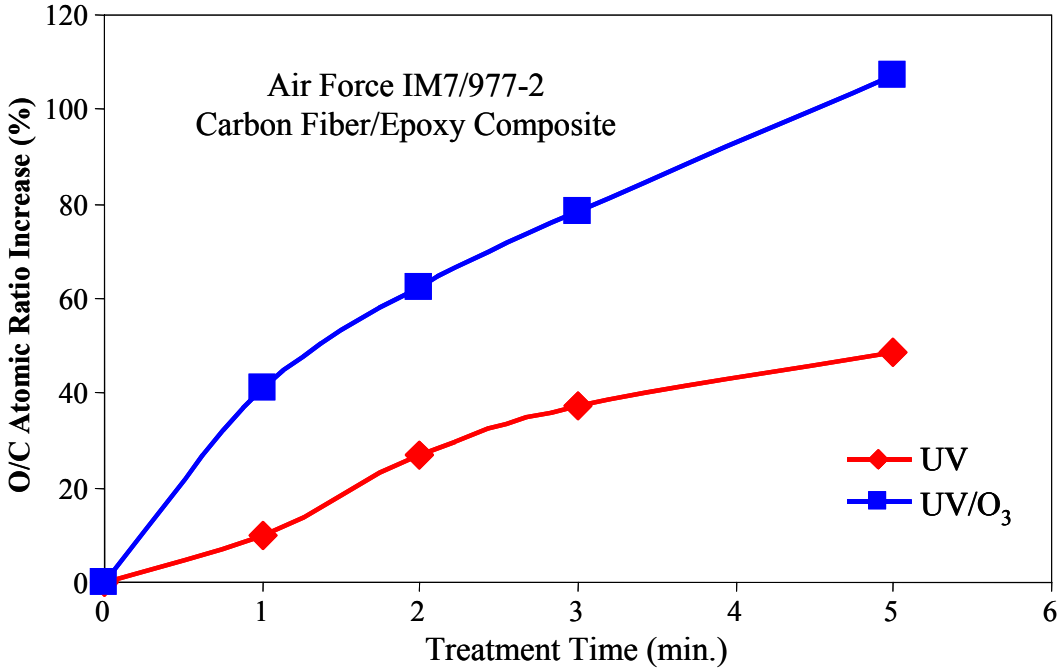

Figure 9: A plot comparing the percentage increase in the O/C ratio as a function of treatment time for UV and UV/O_3 treated IM7/977-2 carbon fiber/epoxy composite.

treatment cases (UV and UV/O_3) the O/C ratio increases linearly as the treatment time increases. These results indicate that the surface becomes more polar as the treatment time increases. In contrast to the AS4/3501 carbon fiber/epoxy composite, there does not seem to be a plateau in the O/C data.

Note that ESEM investigation of both the AS4/3501 carbon fiber/epoxy composite and the IM7/977-2 carbon fiber/epoxy composite did not reveal any exposed carbon fibers, so it is unlikely that the XPS results contain carbon fiber information. (In addition, the small penetration distance of XPS would preclude carbon fiber detection.) To better understand the effects of UV and UV/O_3 treatment of the carbon fiber/epoxy composites the O/C atomic ratios are plotted in Figure 10. The data shows that for both types of composites the use of supplemental ozone caused a significantly more of surface oxidation. In addition, UV/O_3 treatment of the IM7/977-2 composite showed significantly more oxidation compared to the AS4/3501 composite. Some of this increased oxidation level could arise because the IM7/977-2 carbon fiber/epoxy composite had a higher initial surface oxidation.

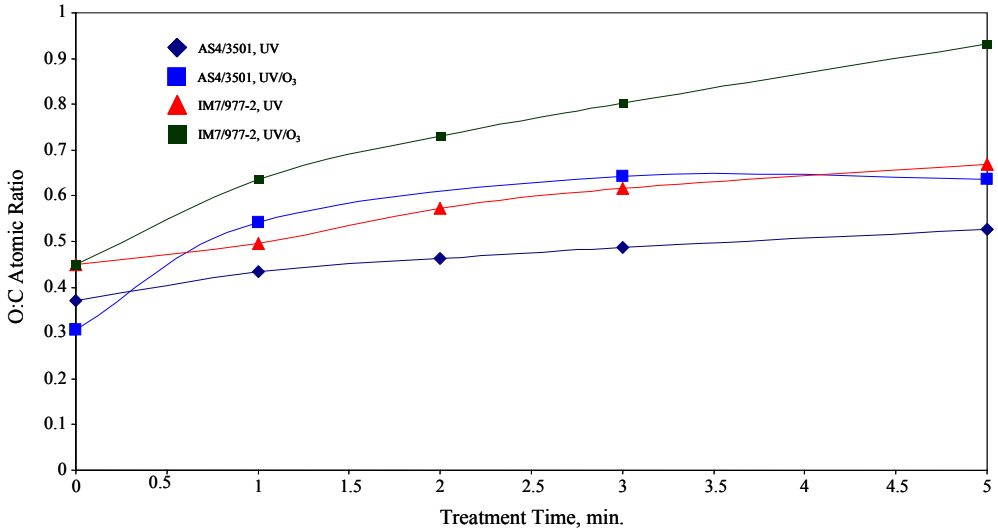

Figure 10: A comparison of the O/C atomic ratios for UV and UV/O_3 treated AS4/3501 and IM7/977-2 carbon fiber/epoxy composites.

Debond Strength

The data in Figure 11 shows the effect of the surface treatment on the debond strength measured using the PATTI test. Though the scatter band is relatively large, there seems to be a slight positive effect for the UV treated specimens and a null effect for the UV/O_3 treated specimens. The large amount of scatter in the treated specimens does not appear in the untreated specimens. No apparent reason for this behavior was found; however, an increase in the heterogeneity of the surface structure (either surface chemistry, morphology, or molecular weight) may create inconsistent failures.

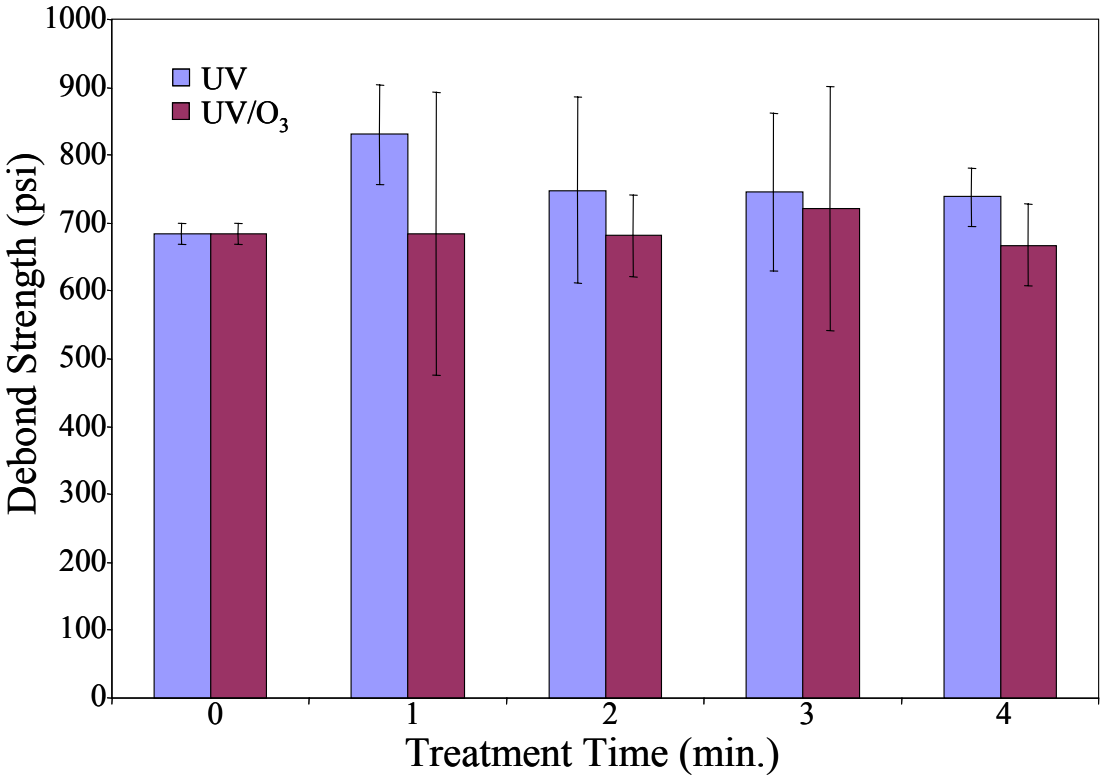

Figure 11: Debond strength (measured using a butt tensile test) of IM7/977-2 carbon fiber composite treated using the RC-747 system.

Fractography

Figure 12 shows ESEM micrographs of the fracture surfaces of as-received IM7/977-2 carbon fiber composites tested in a tensile butt test. Several qualitative points can be made from this examination. First of all the failure surface was heterogeneous with large regions of adhesive epoxy (as shown in Figure 12a) combined with large regions devoid of adhesive epoxy and unremarkable damage to the composite surface. A definite locus of failure is hard to define. It appears that a mixed locus of failure occurs: (1) cohesive within the epoxy adhesive or (2) failure at the adhesive/matrix interface. A comparison between the fracture surfaces for the as-received and treated specimens is shown by the micrographs in Figure 13. In all three cases the response of an island of matrix epoxy to the fracture is illustrated. For the case of the as-received specimen, the matrix material remained unaffected by the adhesive and subsequent fracture. The micrographs in Figure 13a, 13b, and 13c are at comparable magnifications and show dramatically different behavior. In the case of 13b and 13c a crazing type behavior appears on the surface and the island of matrix has been pulled off the composite. In addition to theses differences, the ESEM micrographs in Figure 14 show how the UV and UV/O_3 surface treatments affect the adhesion between the epoxy adhesive and the fibers near the surface of the composite.

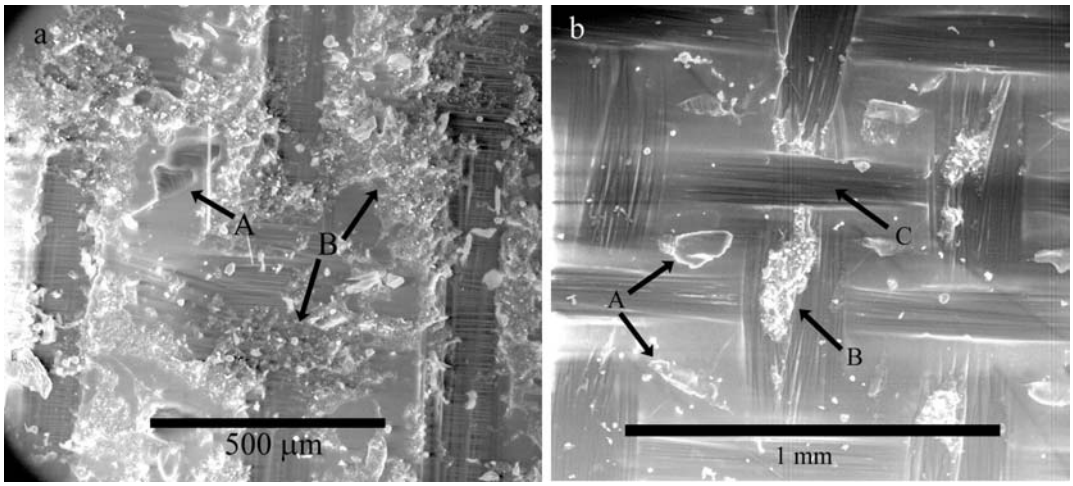

Figure 12: Fracture surfaces of as-received IM7/977-2 showing (a) regions where matrix material was pulled from the composite (A) and large amounts of remnant adhesive (B); and (b) apparent matrix/epoxy interfacial failure (A), a large piece of remnant adhesive (B), and undisturbed fiber region of the composite (C).

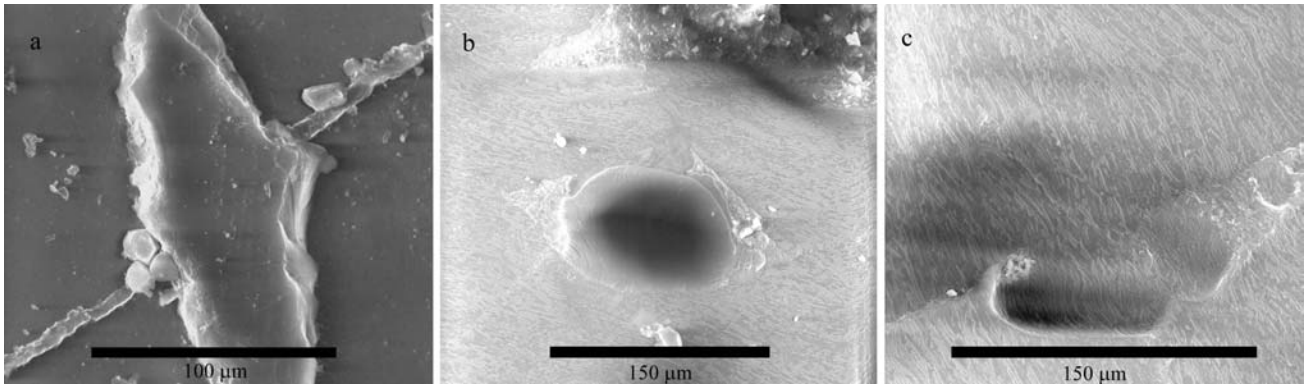

Figure 13: ESEM micrographs showing high magnification images of the fracture behavior of (a) as-received, (b) UV treated for 4 minutes, and UV/O_3 treated for 4 minutes.

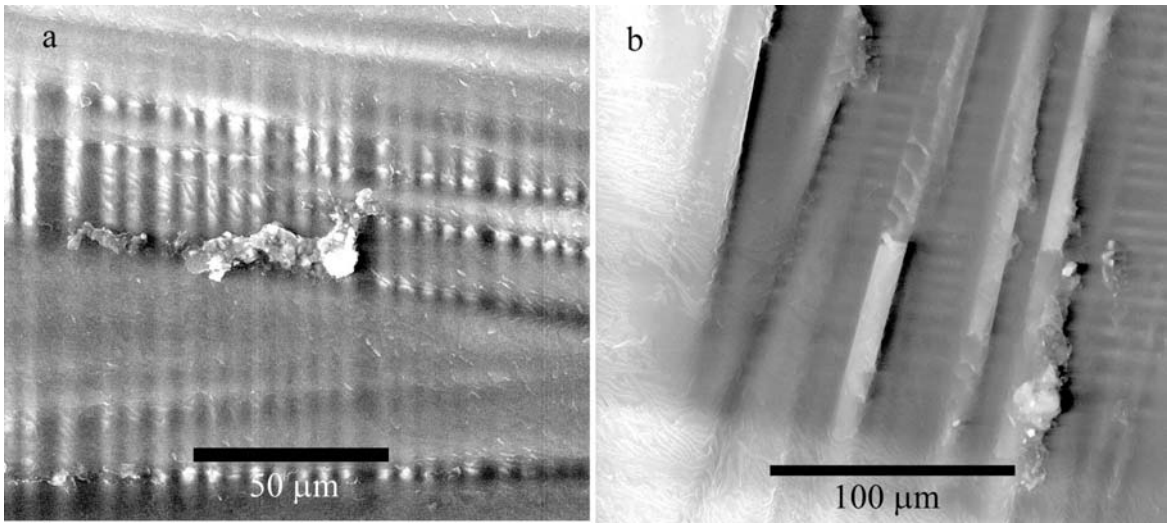

Figure 14: High magnification ESEM micrographs of the fracture surfaces of (a) UV treated IM7/977-2 and (b) UV/O_3 treated IM7/977-2 composites.

Paints. The objective of this portion of the study was to intentionally contaminate painted parts and evaluate the effectiveness of UV and UV/O_3 in removing contaminants. The painted surfaces were contaminated by coating with either hand lotion or a forming oil to simulate an exaggerated amount of contamination.

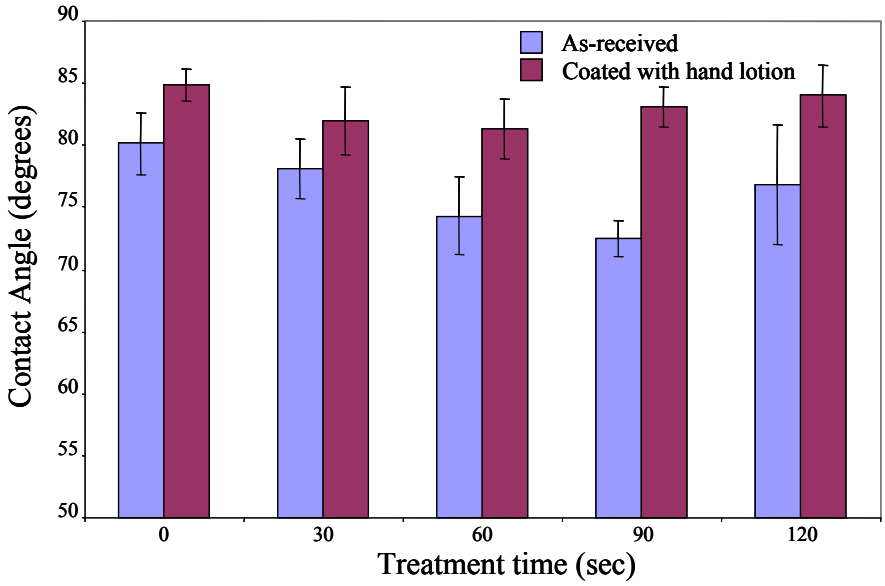

Figure 15: Contact angles for paint on a steel substrate in the as-received condition or coated with hand lotion. The specimens were UV treated using the RC-747 system.

Steel Substrate. The data in Figure 15 shows that UV treating the uncontaminated paint causes the contact angle to decrease to a minimum of 73º for a treatment time of 90 seconds. Treating for over 90 seconds causes the contact angle to increase by 4.5º to 77.5º. A decrease in contact angle followed by an

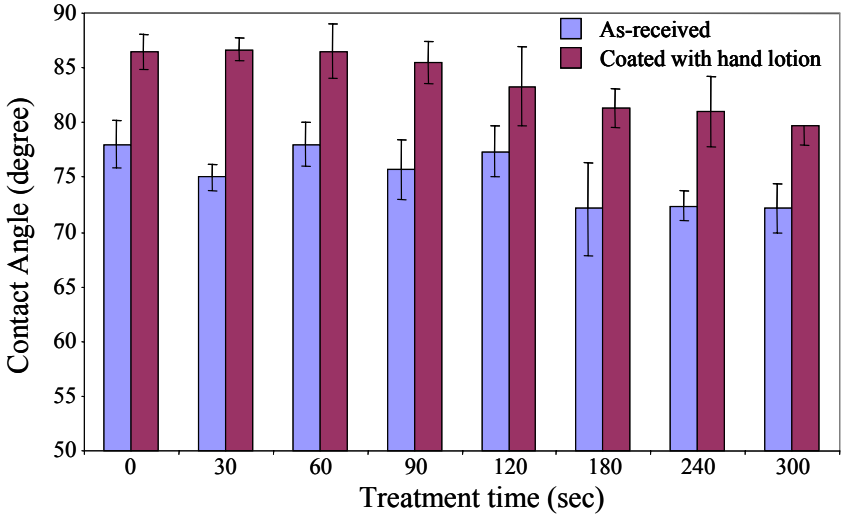

Figure 16: Contact angles for paint on a steel substrate in the as-received condition or coated with hand lotion. The specimens were UV treated using the RC-500 system.

increase in contact angle is not too common. This behavior can occur when non-polar polymer chains rotate to the surface as the temperature increases above the glass transition. A similar, though much less pronounced, contact angle trend is observed for the specimen coated with hand lotion. This behavior may be partially explained by molecular rotations; however, oils and other lubricants in the lotion may be effusing to the surface thereby increasing the hydrophobicity of the surface.

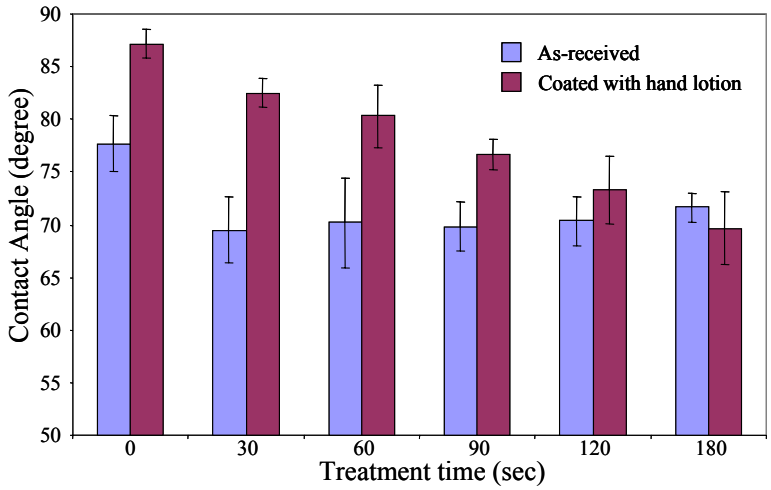

Figure 17: Contact angles for paint on a steel substrate in the as-received condition or coated with hand lotion. The specimens were UV/O_3 treated using the RC-500 system.

Using the RC-500 UV system to irradiate the same types of samples as above resulted in the data plotted in Figure 16. For the as-received specimen the UV treatment causes only a slight decrease in contact angle (77.5º versus 73º) after a treatment time of 180 seconds. These results are similar to the results for the RC-747 system, but the trend is much stronger when using the RC-747 system. The contaminated specimen has an initial contact about 9º greater than the as-received specimen. The contact angle remains constant for UV treatment times of up to 60 seconds. For UV treatments beyond 60 seconds the contact angle begins to decrease. After treating for 5 minutes the contact angle has decrease about 6º to 80º. This minimum contact angle is still well above the contact angle for the as-received specimen (80º compared to 72º).

Figure 17 shows how the wettability of the paint surface changes when treating the surface using the RC-500 system coupled with supplemental ozone. In the case of the as-received system a 30 second UV/O_3 treatment results in a contact angle decrease of approximately 8º. This decrease remains relatively constant for treatment times up to 180 seconds. The use of supplemental ozone causes dramatic changes in the contact angle for the contaminated paint sample. In this case, a strong decreasing trend terminates with a nearly equivalent contact angle as the as-received sample. This trend agrees in general with the data observed in Figure 16 for the UV only treatments. The data indicates that the use of supplemental ozone accelerates the oxidation of the contamination. In addition, these results suggest that the similar levels of hydrophobicity exist, but do not indicate that the same chemistry is present on the as-received and contaminated specimens.

The contact angle results obtained when using the RC-500 and RC-740 UV systems differ significantly. The higher power RC-747 system had a negligible effect on the contamination, yet the RC-500 system reduced the contact angle substantially. The reason(s) for this result are not clear. One reason may be that the contamination thickness was not control sufficiently to make quantitative comparisons between the two treatments.

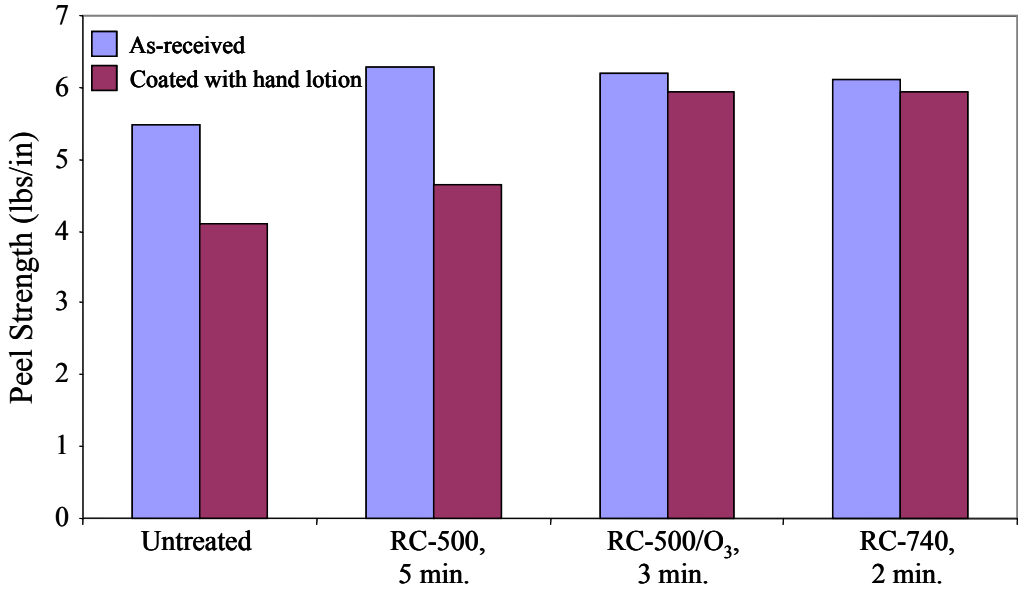

Figure 18: 180 peel test of paint on a TPO substrate.

The data in Figure 18 shows how the peel strength varies as a function of treatment conditions for both as-received and hand lotion coated specimens. The as-received specimens show a small increase in peel strength for UV and UV/O_3 treated specimens. In contrast, the contaminated specimens

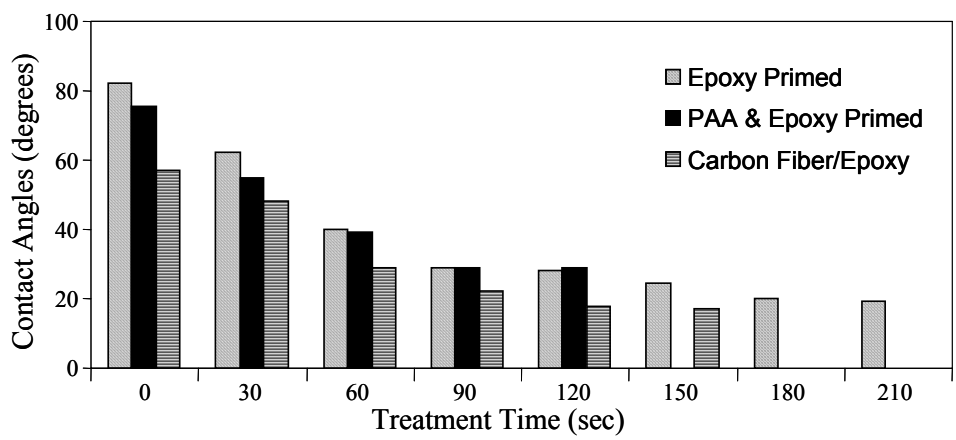

Figure 19: Contact angles as a function of UV treatment time (Fusion 6000 Lamp system).

show a substantial increase in peel strength for specimens treated using the RC-500 lamp with ozone and the RC-740 lamp without ozone.

Epoxy (DGEBA, Diglycidyl ether of bisphenol-A)

Epoxy on Aluminum substrate, Epoxy on Phosphoric Acid Anodized Aluminum, Carbon Fiber Epoxy Composite

Contact Angles. The contact angle as a function of UV treatment time for epoxy specimens is shown in Figure 19. A trend of decreasing contact angle with increasing treatment time occurs for each substrate material. These results indicate that the contact angle is independent of the substrate material. Furthermore, this is a consequence of the relative large thickness of the epoxy covering the substrate and the relatively small penetration depth of the UV light.

In addition to the functional dependence of the contact angle, the initial contact angles are different for different specimens. The reason for this is not know. Presumably the surface conditions are different in some sense. This could include release agents, contaminations, or conditions associated with the epoxy formulation. Regardless of the differences, the results are similar: a dramatic decrease in contact angle is observed.

When the epoxy primed and the PAA and epoxy primed specimens are coated with forming oil and treated using UV light from the Fusion 6000 system the contact angle decreases with increasing treatment time as shown in Figure 20. Though there is an initial difference in contact angle between the as-received and the contaminated specimens the differences disappear after a treatment time of 60 seconds. Furthermore, a contact angle value of approximately 20º is reached for both the epoxy primed

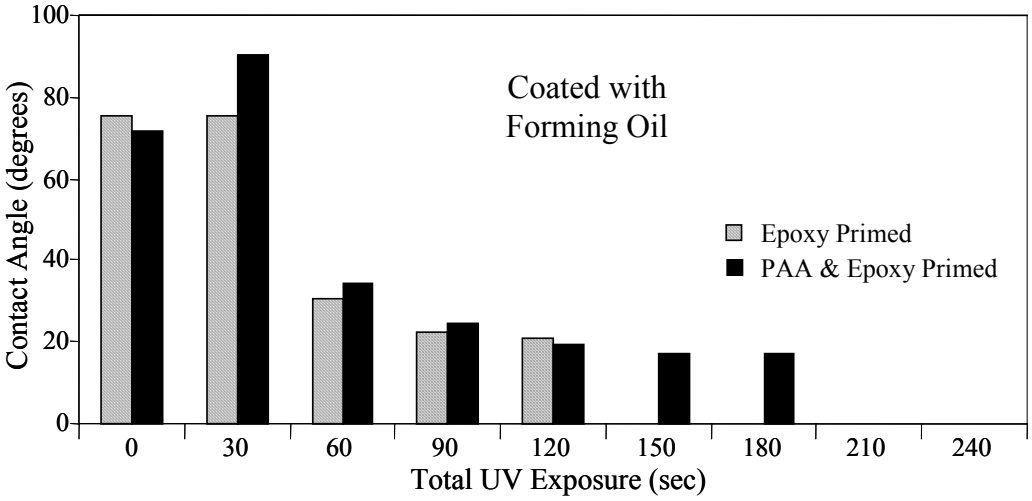

Figure 20: Contact angle of samples coated with forming oil (Fusion 6000).

and the PAA and epoxy primed. These contact angle values are slightly lower than the values determined for the as-received epoxy samples. This means that the UV treatment may be removing and oxidizing the forming oil, but may not be removing all of the oil.

GE 840 Polycarbonate (model thermoplastic material) For reference, the molecular structure of polycarbonate is given in Figure 21. This polymer is made by condensation polymerization, and contains the benzene ring (aromatic structure), which is particularly stable against thermal or oxidative degradation. The chain stiffness is determined by the benzene rings and the substituent groups forming the adjacent part of the chain (attached in the para positions on opposites sides of the rings).

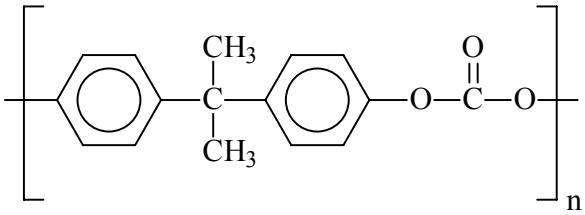

Figure 21: Molecular structure of polycarbonate.

UV interactions with polycarbonate have been studied for many years. In general, UV irradiation of polycarbonate results in the chain scission of the polymer. Chain scission occurs via photolysis of phynel ester linkage and subsequent decarbonylation of the primary radical to yield either a substituted phenoxy end group or a substituted phenyl radical at the point of chain scission. Though the reaction of the polycarbonate with long wavelength light (> 310 nm) is not well understood, when radiated with UV light less than 310 nm the polymer undergoes a photo-Fries rearrangement. When in the presence of oxygen, oxidative reactions also occur.

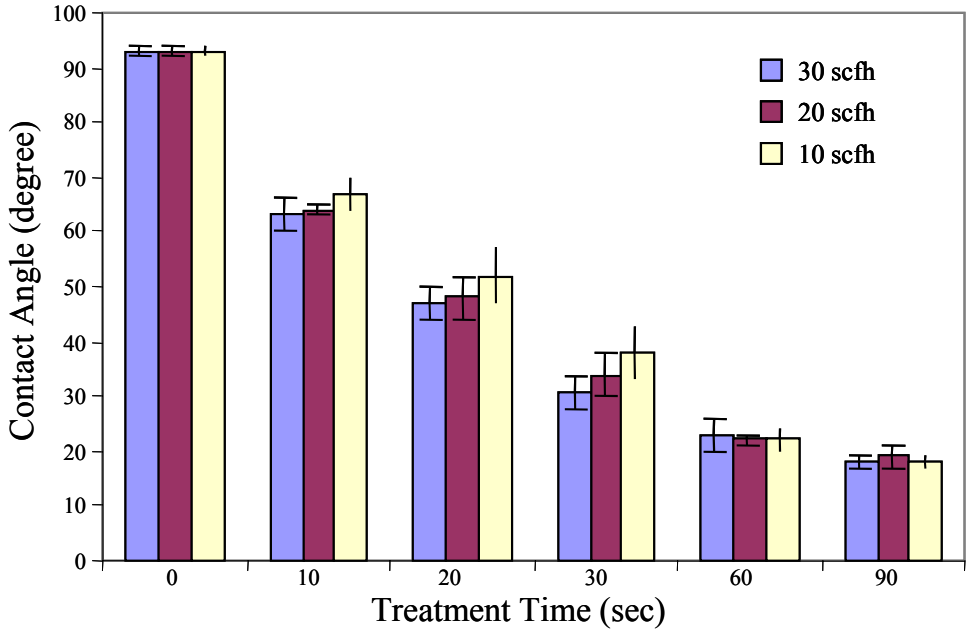

Figure 22: Water contact angle versus treatment time for UV/O_3 treated (RC-747 120 Hz) polycarbonate as a function of O_3 flow rate.

To better understand the effect of the ozone in the presence of UV light, the ozone flow rate was varied and the resulting contact angle measured as a function of UV treatment time. Using the RC-747 system, Figure 22 compares how the ozone flow-rate —at a concentration of 720 ppm— influences the contact angle. The data reveals that as the treatment time increases the contact angle smoothly decreases to approximately 20º after 1.5 minutes of UV/O_3 treatment. Also, the contact angle is seen to be weakly dependent on flow rate. In general, changing the ozone flow rate should change the mass transfer coefficient between the PC and the gas. A higher ozone velocity (higher flow rate) should increase the mass transfer. Since the data shows little, if any, difference in contact angle for the different flow rates, within this range of flow rates there is no mass transfer limitation.

The contact angle of PC as a function of ozone concentration at a constant flow rate of 30 scfh is

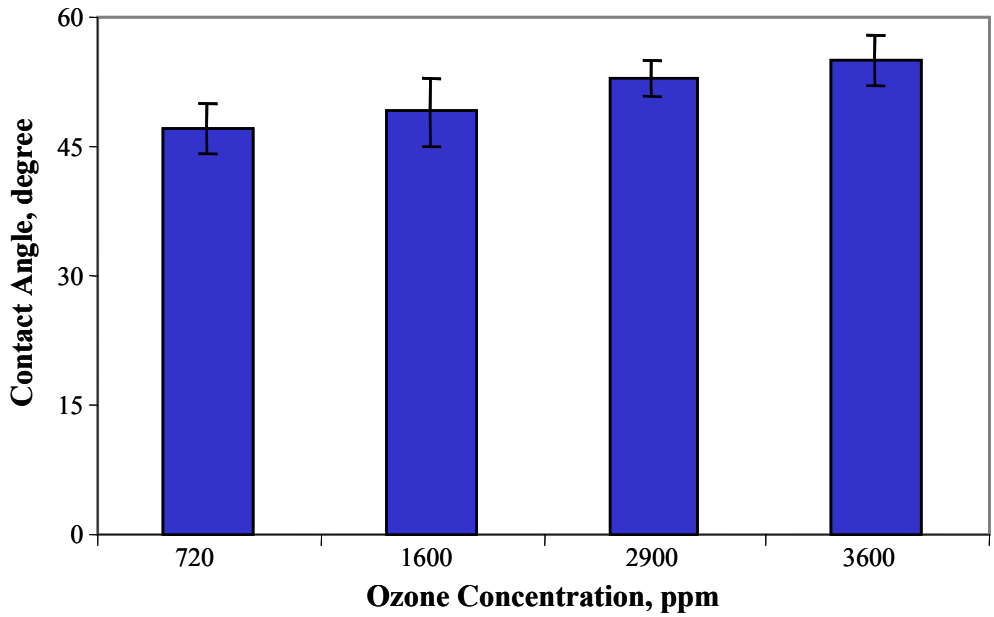

Figure 23: Plot showing the effect of ozone concentration (RC-747, 120 Hz) on the contact angle for polycarbonate.

shown in Figure 23. The data shows a slight increase in contact angle as the ozone concentration increases. This indicates that the surface is becoming more hydrophilic as the ozone concentration increases. The contact angle data reflects the complicated and dynamic processes that occur during the UV/O_3 treatment of PC. Ozone is one of the strongest oxidizers and reactions between the ozone and PC would be anticipated even in the absence of UV radiation. In addition, the effects of UV and PC interactions have been presented. The increase in hydrophillicity for higher ozone concentrations results from a strong absorptive interaction between the incident UV and ozone in the 220-280 nm wavelength band. The attenuated UV irradiation is not able to generate a sufficient number of free radicals to functionalize the PC surface and promote wetting. Therefore optimization procedures should take into account the UV/O_3 absorption interaction.

Figure 24 shows the contact angle variation for low ozone concentrations for a 30 second UV/O_3 treatment. Individual contact angles are shown for each concentration. The data shows a large amount of scatter at low concentrations. As the ozone concentration increases, the scatter decreases. For ozone concentrations of 400 ppm and above, the data points collapse plateau at a contact angle of approximately 38º. The scatter in the data for low ozone concentrations probably results from poor sample coverage.

To help understand how the lamp-to-sample distance affects the UV treatment of PC (and other materials), the irradiant power as a function of distance from the lamp (at a wavelength of 254 nm) is plotted in Figure 25. Note that the total radiation efficiency in terms of UV energy output is affected by the operating power level of the lamp. In this case the RC-747 lamp system is being operated at a frequency of 120 Hz. Also, UV lamps emit not only ultraviolet light, but also visible light, and wavelengths in the infrared spectrum. In fact, all lamps emit approximately 20% ultraviolet light, 60% infrared light and 20% visible light. It is therefore important that when selecting a lamp and using a lamp system the output in the ultraviolet spectrum should be closely examined. The data in Figure 25 were collected using a cosine collector equipped with a 254 nm filter. Figure 25 shows the power very close to the lamp is high and increases to a peak at a sample-to-lamp distance of 1 inch. Beyond one inch the power drops significantly as the sample-to-lamp distance increases. These results suggest that a processing compromise can be made between long treatment times or high concentrations of ozone.

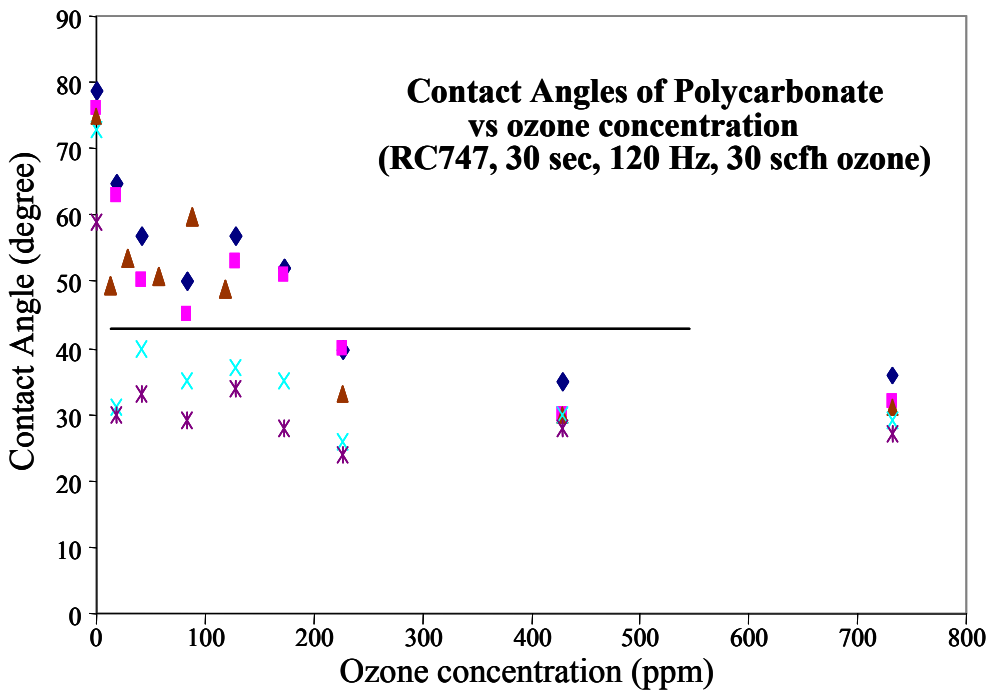

Figure 24: Water contact angles versus ozone concentration for polycarbonate treated with the RC-747 system. (Note data points represent individual contact angle measurements.)

As further evidence of the effect of the lamp-to-sample distance the data in Figure 26 plots the contact angle versus total irradiance (power integrated over time) for a range of sample-to-lamp distances for a UV treatment. At low irradiances, high contact angles for all lamp-to-sample distances. As the irradiance increases, two different curves appear. First for distances of 3 inches and greater, the contact angles are approximately the same. For samples at distances of 1.25 and 2 inches, the contact angles are significantly lower than the contact angles at larger sample-to-lamp distances. As the irradiance increases, all curves collapse to the same contact angle, independent of sample-to-lamp distance. This suggests that given a long enough the same contact angle can be achieved independent of

the instantaneous power. Furthermore for optimum effectiveness —in terms of contact angle— the sample-to-lamp distance should be between 1 and 2 inches.

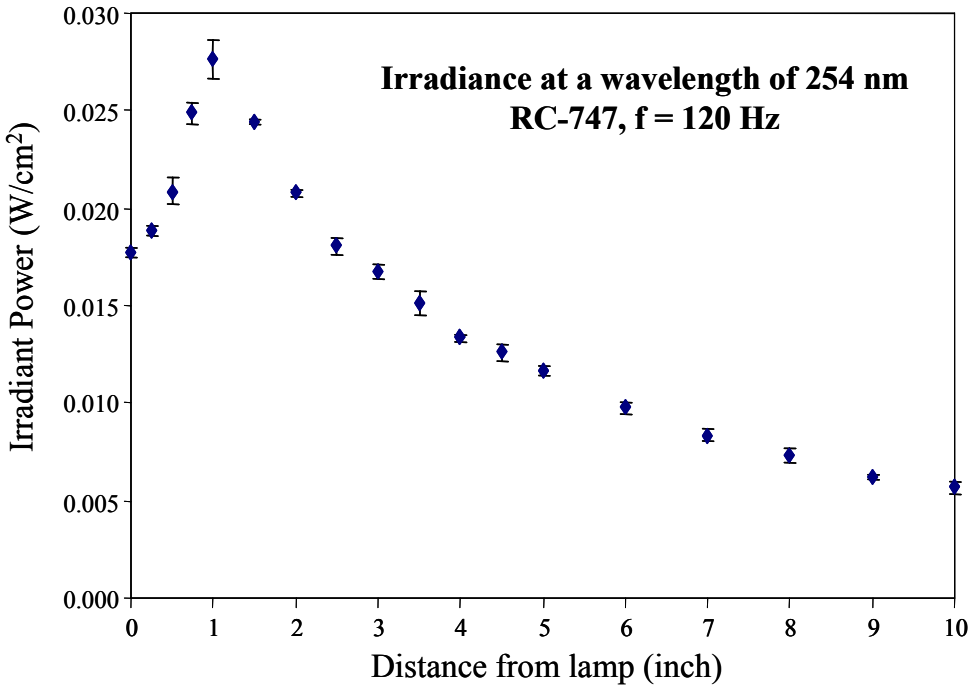

Figure 25: A plot of the irradiant power as a function of distance from the lamp for the RC-747 lamp system.

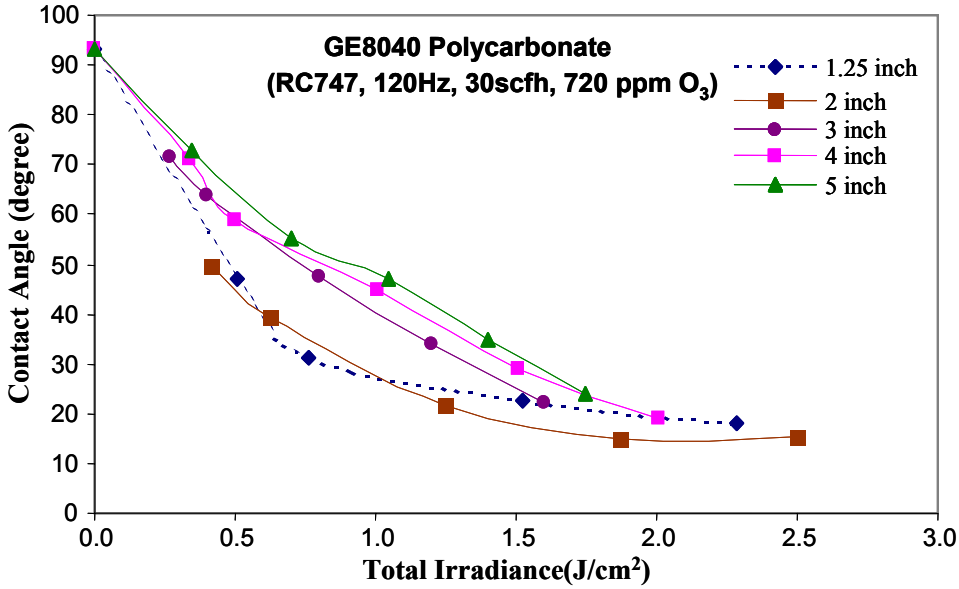

Figure 26: A plot illustrating how the contact angle varies as a function of total irradiance for a range of sample-to-lamp distances.

The sample-to-lamp distance data from Figure 26 is replotted in Figure 27 to further illustrate the independent character of the contact angle on total irradiance. The black line drawn through the data provides a guide showing how the data collapses for higher irradiances.

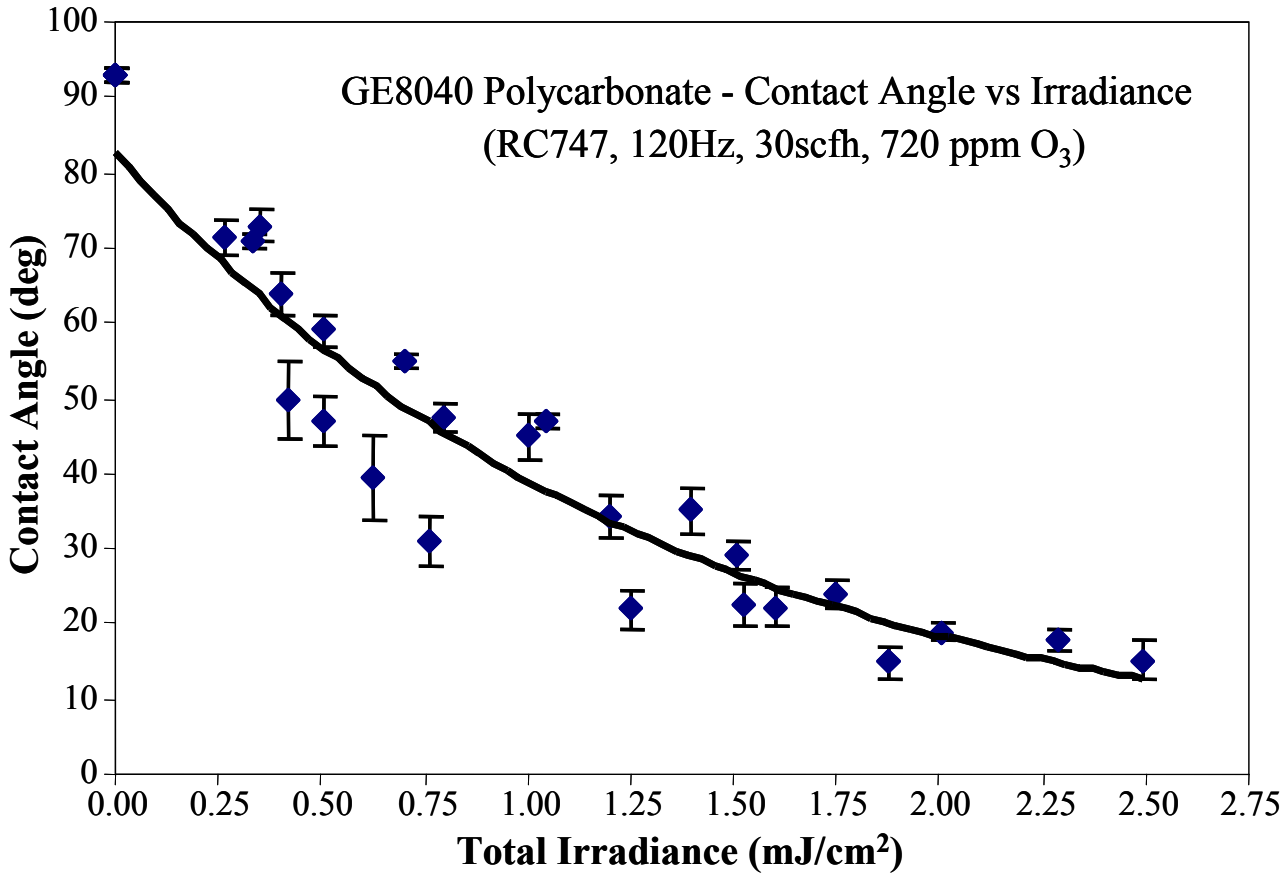

Figure 27: The same data as in Figure 26 —replotted with averaged values and only one data symbol— illustrating the universal character of the contact angle total irradiance dependence.

As discussed in the experimental methods section, the work of adhesion can be calculated using the contact angle information. Calculating the work of adhesion from the data plotted in Figure 27 allows the work of adhesion versus total irradiance to be plotted in Figure 28. The data shows that the work of adhesion for UV/O_3 treated PC increases in a smooth manner for increasing total irradiance. The work of adhesion appears to saturate at a value of 140 mJ/m^2.

In addition to the work of adhesion the acid-base total surface energy and the individual acid/base components of the surface energy of the UV/O_3 treated PC was calculated and plotted as a function of irradiant energy in Figure 29. (Note the different scales on the right- and left-hand side vertical axis.) The data shows that the total surface energy increases during irradiation. In addition, there is a large increase in the base component of the surface energy and only a very slight change in the acid component. As might be expected, there was no change in the Lifshitz-van der Waals component.

The polar and dispersive components of the surface energy were also calculated from contact angle measurements. The results are plotted in Figure 30. Similar to the acid-base analysis, the total

surface energy increases with increasing total irradiance reaching a value of 60 mJ/m^2 for a total energy of 2000 mJ/cm^2. The polar component of the surface energy increases in a linear manner to a maximum

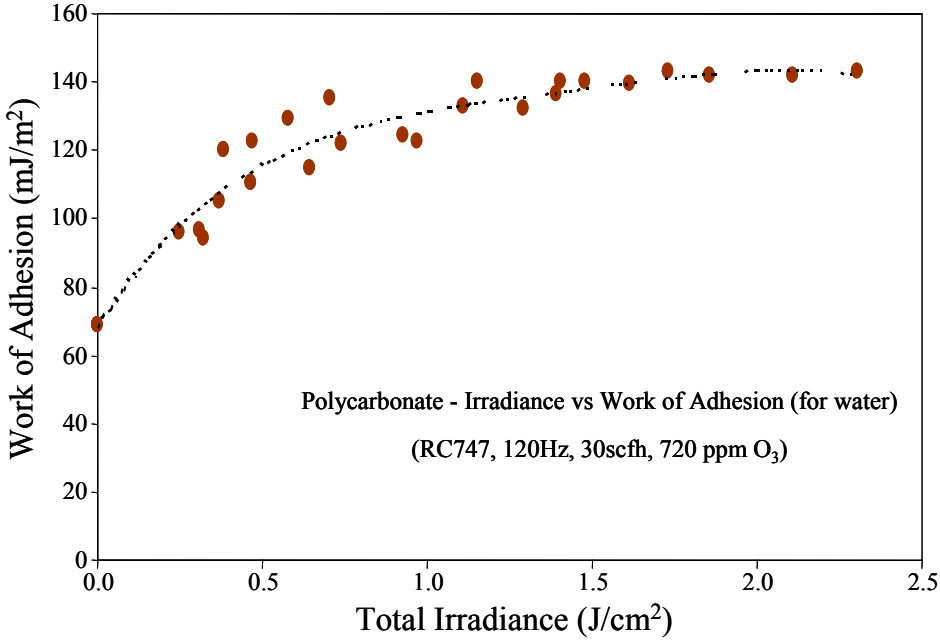

Figure 28: This data shows how the work of adhesion varies according to the total irradiance (energy density).

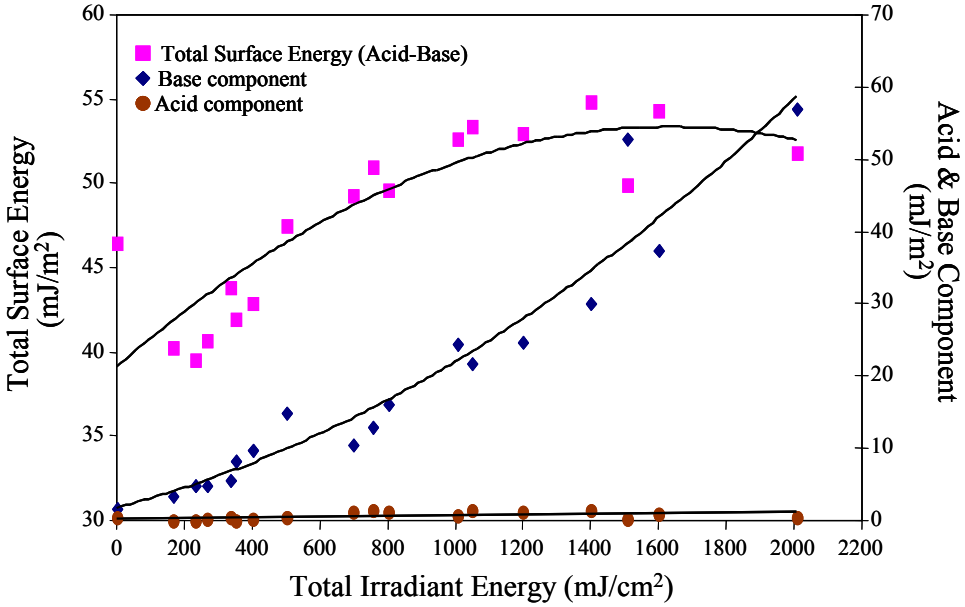

Figure 29: Plots comparing the total surface energy and the acid-base component versus total irradiant energy for PC irradiated using the

value of 34 mJ/m^2. In contrast, the polar component of the surface energy shows a slight decrease as the total irradiant energy increases.

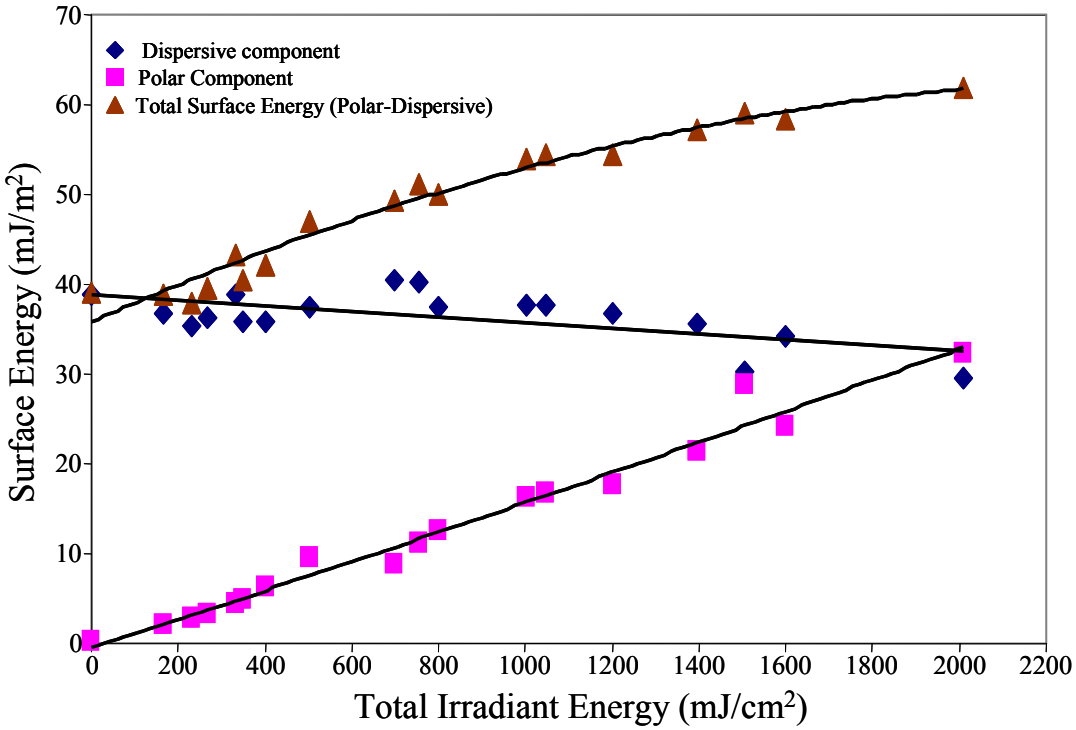

Figure 30: A plot of the surface energy, and components, versus the irradiance for UV/O_3 treated polycarbonate.

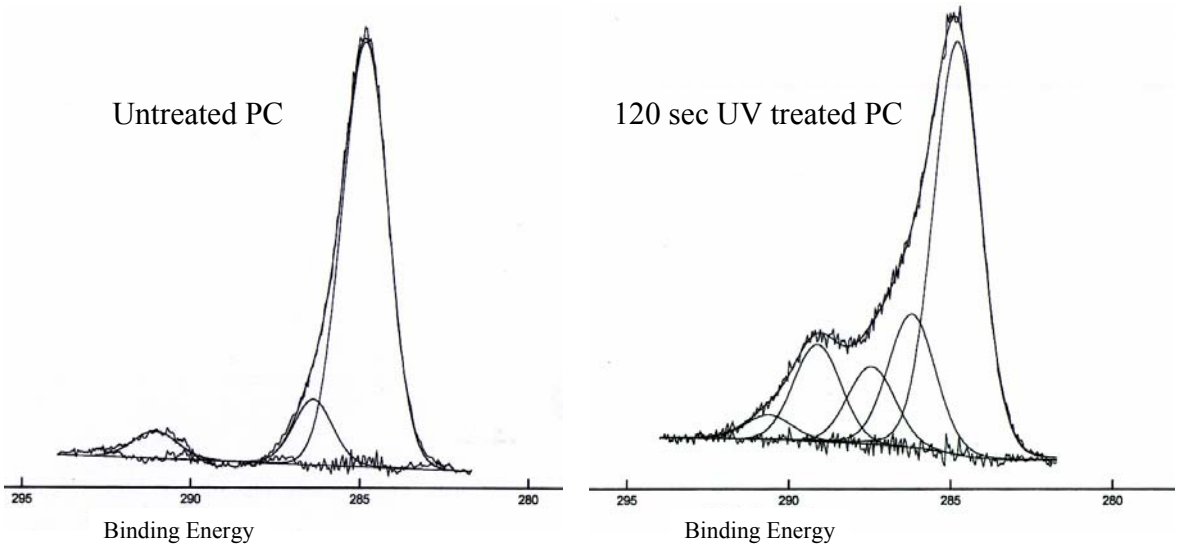

Figure 31: Example of C1s peak deconvolution of PC for untreated and UV treated polycarbonate.

An XPS investigation of UV treated PC as a function of total irradiant energy provides insight into the effectiveness of generating surface functional groups. Figure 31 shows how the C1s signals of the untreated PC are deconvoluted with 3 Guassian peaks positioned at 284.7, 286.11, and 290.9 eV.

The peaks can be assigned to C-C, C-O and O=C=O (carbonate bonds), respectively. A similar analysis of the O1s peak for untreated PC is deconvoluted with 2 Gaussian peaks located at 532.1 and 533.8 eV corresponding to C=O (carbonyl, ether) and OH (alcohol), respectively. Upon UV treatment the C1s peak changes significantly with irradiant energy. For a UV treatment time of 120 seconds the C1s peak shown in Figure 31 is deconvoluted into 5 peaks are positioned at 284.7 (C1), 286.11 (C2), 287.5 (C3), 289.8 (C4), and 290.9 (C5) eV. The C1 peak is assigned to C-C bonds, the C2 peak is assigned to C-O bonds, the C3 peak is assigned to C=O (carbonyl) groups, the C4 peak is associated with the O-C=O (carboxyl) groups, and the C5 peak is assigned to the O=C=O (carbonate) groups.

A summary of the XPS investigation is provided by the data in Table IV. In this table the percentage of surface functional groups is given as a function of irradiant energy (measured at a wavelength of 254 nm). The C1s data indicates a monotonic decrease in the concentration of C-C bonds as the irradiant energy increases. The oxygen containing functional groups shows a general increasing trend, while monotonic increases are observed for the carboxyl and carbonate groups. In particular, the C-O groups appear to saturate at about 18%.

Table IV. XPS Spectra of UV Treated Polycarbonate

	C1s					O1s	
Irradiant Energy (mJ/cm^2)	**284.7**	**286.11**	**287.5**	**289.8**	**290.9**	**532.1**	**533.8**
0	**83.43**	**11.43**	**0.00**	**0.00**	**5.14**	**33.33**	**66.67**
167	**77.75**	**16.85**	**1.13**	**1.13**	**3.14**	**33.93**	**66.07**
335	**71.55**	**15.04**	**5.09**	**4.28**	**4.04**	**48.28**	**51.72**
502	**67.03**	**17.00**	**6.07**	**6.36**	**3.54**	**47.79**	**52.21**
753	**61.27**	**16.71**	**8.66**	**9.49**	**3.86**	**43.02**	**56.98**
1004	**61.15**	**18.89**	**8.25**	**9.00**	**2.70**	**56.07**	**43.93**
1506	**55.45**	**18.78**	**8.27**	**15.01**	**2.49**	**50.49**	**49.51**
2008	**55.60**	**18.19**	**10.12**	**12.59**	**3.51**	**54.47**	**45.53**
	C-C	**C-O**	**C=O**	**O-C=O**	**O=C=O**	**C=O**	**OH**

The functional groups were identified by the O1s behavior in a similar manner to the C1s groups. Initially, the PC surface is populated by alcohol groups (OH). As the irradiant energy increases, the OH groups decrease while the C=O groups increase substantially even for low irradiant energies. In this case the C=O and OH values seem to saturate at around 50%.

To further illustrate the effectiveness of UV treatment imparting polar functional groups to the surface of PC, the oxygen-to-carbon ratio data was plotted as a function of total irradiance in Figure 32. The data shows a smooth increase in the oxygen-to-carbon ratio to an apparent plateau at a ratio of slightly less than 0.50. Table V lists the exact values of the atomic percent of carbon and oxygen present on the surface of the PC as a function of total irradiant energy. The data indicates that the oxygen concentration peaks at approximately 30%. This data shows the same trend as the acid-base surface energy analysis.

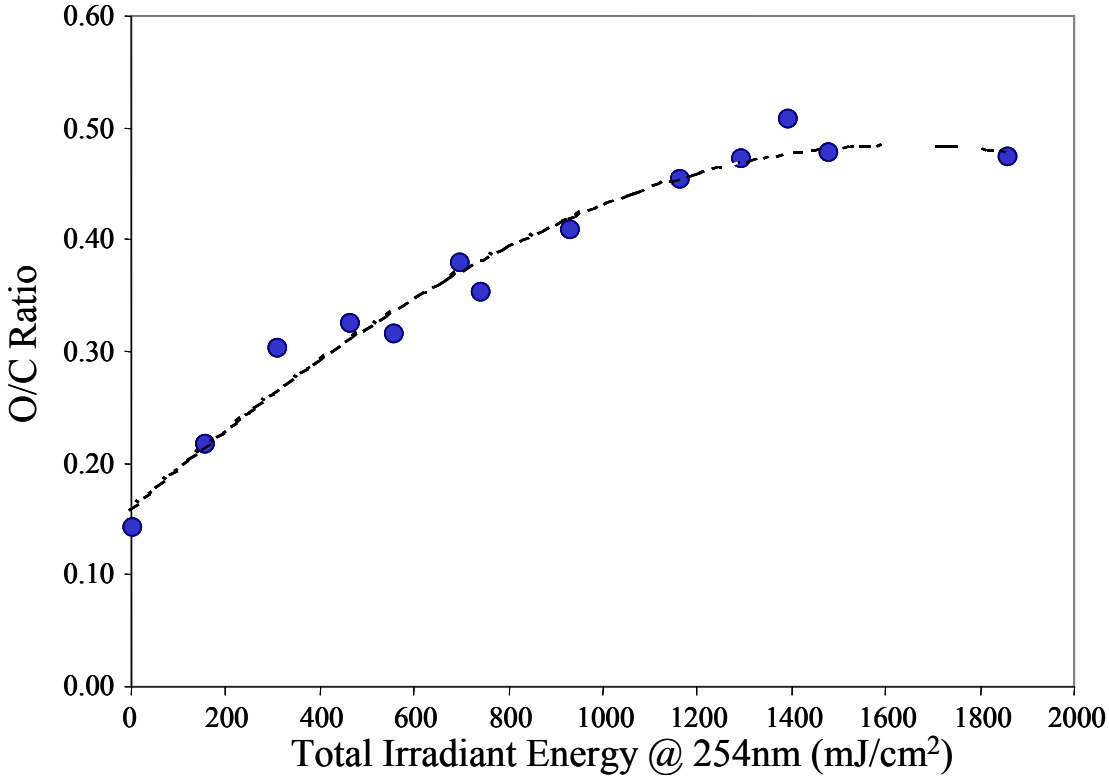

Figure 32: A plot of the oxygen-to-carbon ratio as a function of the total

Table V. Carbon and Oxygen Surface Concentration on UV Irradiated Polycarbonate

Irradiant Energy (mJ/cm^2)	C	O	O/C
0	87.6	12.4	0.14
167	82.2	17.8	0.22
335	76.8	23.2	0.30
502	75.5	24.5	0.32
753	72.6	27.4	0.38
1004	71.0	29.0	0.41
1506	66.4	33.6	0.51
2008	67.9	32.1	0.47

Conclusions:
Research completed under this SERDP project has shown that a very short application of pulsed UV light under ambient atmospheric conditions can provide beneficial surface chemical changes on the surface of plastics, composite materials and metals. This surface treatment can be applied to various materials in use in the DoD inventory for cleaning and preparing their surfaces for the application of and adhesive bonding of adhesives, paints and other coatings to non-metallic and metallic surfaces. Currently used techniques can be time consuming and often require the use of chemicals and other methods to treat the surfaces. Current methods often release quantities of air pollutants including polymers, hydrocarbons and other hazardous materials. The method of using pulsed UV light to treat surfaces can perform the required surface preparation for cleaning and chemical modification of surfaces at a very low cost and with much less release of toxic materials.

The advantages of the Xenon pulsed UV technology are low heat generation and the reduction of the creation of potentially toxic and hazardous byproducts. The development of a process model as well as a data base of the optimum conditions for surface treatment of various materials has provided a critical factor necessary to insure success of this technology in the commercial marketplace. The data and model that is developed will be able to provide information on the best wavelengths, energy levels and exposures needed to prepare various surfaces for surface treatment. This data will enable a manufacturer to fabricate pulsed UV lamp systems tailored for specific applications and also to advise our customers on the best way to treat surfaces.

At this juncture in the research project, it has been demonstrated that the UV treatment process is:

- A new, alternative, environmentally benign, surface pretreatment process for treating the majority of polymer, plastic and polymer composite surfaces using ultraviolet light.
- The non-contact process is adaptable to treat flat or convoluted external surfaces and has the potential to require exposures of less than sixty seconds to produce significant increases in wettability and adhesion of paints and adhesives to treated surfaces.
- The UV process is environmentally benign and has a low environmental impact since it does not create or use VOC's or create suspended airborne particulates.
- The process is extremely easy to implement since it requires only a source of power and does not use any materials or consumables to achieve its result.
- A process comparison and cost analysis of the UV process indicates that this new technology is can be implemented for the cleaning and pretreating of surfaces for painting and adhesive bonding at a cost of ~$0.01 per square foot at high speed treatment times ~ 60 seconds.
- The process has a low capitol investment requirement
- The process can be easily integrated into existing manufacturing or depot environments
- Special Focus on Defense Industry
    - Multiple materials (structural, stealth, electronic… and platforms ground, ship and air)
    - Applications can extend from the simple to the complex (e.g. removal of oils residue or mold release….surface treatment for adhesive bonding or painting)
    - Technology can support rigorous requirements, cost reduction pressures, lead to new technological innovations.

Transition Plan: *(an outline as to how the technical results are/should be transitioned, including critical paths)*

A commercial partner, Xenon Corporation (a small business), has collaborated on this project and provided technical and financial assistance on the pulsed UV process related to issues that require resolution as a precondition for commercialization of this process and transition to the manufacturing arena. Xenon produces a line of pulsed UV lamps that are used in the medical industry and has the know-how and interest to can scale up this system to meet the volume, price and productivity needs of high speed processing in the durable goods and automobile industry. Xenon Corporation has concluded that with the results from this proposed collaborative project, they can scale up this system to meet the volume, price and productivity needs and produce systems for location in depots for DoD applications.

The development of a process model as well as a data base of the optimum conditions for surface treatment of various materials will assist Xenon in transitioning this process to market. The data and model will enable Xenon to provide information on the best wavelengths, energy levels and exposures needed to prepare various surfaces for surface treatment. This data will enable Xenon Corporation to fabricate pulsed UV lamp systems tailored for specific applications and also to advise our customers on the best way to treat surfaces.

MSU owns the intellectual property associated with this technology and would provide a Business Development Team composed of the following personnel:

Louis Panico, President and CEO of Xenon Corporation

Bradley T. Shaw, Adjunct Professor of Marketing, The Eli Broad School of Business, Michigan State University --- Completed Business Opportunities (Ultraviolet Light Surface Treatment Market Analysis), December 15, 2000

Mark H. Clevey, Vice President, Small Business Association of Michigan --- Specialist in High Tech Business Development; Business & Commercialization Plan Reviewer, NIST-ATP, NSF Phase II SBIR/STTR, EPA Phase II SBIR; 5 National Awards for expertise in Entrepreneurialism.

Loch O. McCabe, President, Shephard Capital Ventures, Ltd. --- Founder, Environmental Capital Network; Commercialization Plan Reviewer, EPA Phase II SBIR.

The transition plan would be constructed and implemented by the MSU Business Development Team. In particular their focus would be on the following:

1. Technology Risk - *does the technology work as predicted;*
2. Manufacturability Risk - *can the technology be manufactured reliably and at a sufficiently low cost;*
3. Marketability Risk - *are there customers for the process, beta test sites;*
4. Management Risk - *is the management team capable of building a large and profitable company; and finally*
5. Market Growth Rate Risk - *is the market potential sufficient to build a large company in a five year time horizon.*

Recommendations:

UV processing of materials in DoD facilities would most likely be done by an established DoD depot contractor who would purchase an UV production system designed and assembled (turnkey) by a UV systems integrator. Xenon Corporation would work with the systems integrator and MSU to achieve the optimum performance for the applications. This is the key element of know-how relative to the new technology. The other elements of the system are largely off the shelf items and relatively start-forward. It is assumed that the first customer will need to time the processes cycle time and surface finish at their facility on a full part. SERDP would be asked to assist in the development of follow-on technological innovations.